Preparation and characterization of nanocomposite thin films for polymer electronics

MSc. Bita Ghasemi, Ph.D.

Doctoral Thesis Summary

Tomas Bata University in Zlín

Tomas Bata University in Zlín
Centre of Polymer Systems

Doctoral Thesis Summary

Preparation and characterization of nanocomposite thin films for polymer electronics

Příprava a charakterizace nanokompozitních tenkých vrstev pro polymerní elektroniku

Author:	MSc. Bita Ghasemi, Ph.D.
Degree programme	P3972 Nanotechnology and Advanced Materials
Degree course:	3942V006 Nanotechnology and Advanced Materials
Supervisor:	prof. Ing. et Ing. Ivo Kuřitka, Ph.D. et Ph.D.
Consultant:	Ing. Pavel Urbánek, Ph.D.
External Examiners:	RNDr. Eva Majková, DrSc.
	prof. Ing. Petr Slobodian, Ph.D.

Zlín, April 2024

Published by **Tomas Bata University in Zlín** in the Edition **Doctoral Thesis Summary.**
The publication was issued in the year 2024

Key words in Czech: *tenké kompozitní vrstvy, strukturní uspořádání, J- a H-agregáty, nanoplnivo, MEH-PPV, PLED*

Key words: *F8BT; thin composite films; structural ordering; J- and H-aggregates, Nanofiller, MEH-PPV, PLED*

ISBN 978-80-7678-257-0

Acknowledgment

First and foremost, I would like to praise and thank God, the Almighty, who has granted countless blessings, knowledge, and opportunity to me so that I have been able to achieve my goal and be successful in this part of my life's journey.

Words cannot express my gratitude to my supervisor, prof. Ing. et Ing. Ivo Kuřitka, Ph.D. et Ph.D. for his continuous support during my doctoral study. His patience, motivation, immense knowledge, and guidance helped me in all the time of research.

I am deeply grateful to my advisor, Dr. Ing. Pavel Urbánek, for his treasured support, which was influential in shaping my experiment methods and critiquing my results. His great knowledge and plentiful experience have encouraged me in all the time of my academic research and daily life.

I would like to express my sincere gratitude to my colleague Ing. Jakub Ševčík, Ph.D., for his insightful comments and suggestions. I also appreciate all the support I received from the rest of my colleagues Dr. Ing. Barbora Hanulíková, Dr. Ing. Michal Urbánek, Ing. Milan Masař, Ph.D.

I extend my deepest appreciation to Ing. Jan Antoš, Ph.D., whose generosity and expertise have been invaluable during the journey of writing this thesis. his willingness to share his time and knowledge have significantly enriched the quality of this work. The collaborative spirit demonstrated by Honza not only made the research process more enlightening but also reminded me of the strength found in unity. I am sincerely grateful for his guidance, and encouragement.

I would like to offer my special thanks to Dr. Vojtech Nádaždy from the Institute of Physics of the Slovak Academy of Sciences in Bratislava, who founded the unique energy-resolved electrochemical impedance spectroscopy method and developed the first apparatus hitherto unavailable in any other laboratory. I would like to extend my sincere thanks to Dr. Karol Végsö and Dr. Peter Šiffalovič for their contribution to GIWAXS measurement.

There must be an extraordinary thanks to doc. RNDr. Jana Toušková, CSc., and RNDr. Jiří Toušek, CSc., from the Department of Macromolecular Physics, Faculty of mathematics and physics, Charles University. Their support during my stay in Prague, as well as the discussions of obtained results, are greatly acknowledged.

This Thesis was supported by internal grant agency of TBU in Zlín projects no. IGA/CPS/2020/003, no. IGA/CPS/2021/002, no. IGA/CPS/2022/002, and no. IGA/CPS/2023/006, in which I was working as a member of team. I also express my gratitude for the financial support provided to my research by acknowledging the funding providers in the appropriate sections of my published or submitted papers whenever feasible. In this context, I would like to extend my thanks to the Centre of Polymer Systems at Tomas Bata University in Zlín for their financial support during my studies.

Abstrakt

Tato práce přináší studium netriviálních vztahů mezi tloušťkou polymerních filmů a jejich elektrickými a optoelektrickými vlastnostmi. Tyto vztahy byly studovány na polymeru poly(9,9-dioctyfluorene-altbenzothiadiazole), F8BT, kde bylo jasně prokázáno, že tloušťkový parametr výrazně ovlivňuje uspořádanost tenkého filmu a tím i výsledné chování polymeru.

Další výsledky, získané během studia chování nanokompozitních tenkých vrstev, jasně prokázaly, že přidání nevodivých nanočástic do polymerní matrice poly[2-methoxy-5-(2-ethylhexyloxy)-1,4-phenylenevinylenu] (MEH-PPV) způsobilo rozuspořádaní polymerních řetězců a s tím spojené efekty, jako je vznik nových elektronových stavů v zakázaném pásmu, pokles mobility náboje a zkrácení difúzní délky excitonu. Tyto změny pak ovlivnily maximální svítivosti a celkovou proudovou účinnost připravených diod, v nichž byl tento nanokompozit použit. Na druhou stranu přídavek nanočástic vedl k prodloužení operační životnosti diod.

Abstract

This research demonstrated that the optoelectronic characteristics and structural (dis)order in thin conductive polymer films have a non-trivial thickness dependency, studied for poly(9,9-dioctylfluorene-*alt*-benzothiadiazole), F8BT thin films.

Furthermore, new results obtained during the investigation of the behaviour of nanocomposite thin films made of poly[2-methoxy-5-(2-ethylhexyloxy)-1,4-phenylenevinylene] (MEH-PPV) and Al_2O_3 nanowires demonstrated that the addition of a nanofiller can play a significant role, resulting in the creation of new energetically favourable states in polymer chains. These states preferentially emerge due to the disordering induced by nanofiller. The change of thin polymer structure correlates with the final properties of nanocomposite material, such as density of states in the band gap, reduction in charge mobility, and shortening of the exciton diffusion length. These changed parameters result in the reduction of the maximum luminance and the current efficiency of the prepared diodes. On the other hand, the nanofiller addition contributed to an increase in the operational lifetime of the diodes.

CONTENT

1. INTRODUCTION

1.1 Conjugated polymers

Conjugated polymers/inorganic hybrid nanocomposites are now extensively used as an active layer in optoelectronic devices such as smart microelectronics, photovoltaic cells, sensors, photodiodes, and organic light-emitting diodes (OLEDs) [1]. When compared to equivalent inorganic counterparts, their distinguishing characteristics, such as ease of processing, low toxicity, a high optical absorption coefficient ($\sim 10^5$ cm^{-1}), energy tunability (2.5-4 eV), and cheaper cost and weight, make them a potential candidate in this respect [2,3]. A polymer (a substance composed of a long chain of molecular structures) is primarily an insulator. The notion that polymers or plastics may carry electricity is seen to be ludicrous. Their vast applicability as an insulating material is the primary reason they are investigated and developed. In reality, these materials are extensively utilized for covering copper wires and fabricating the outside frames of electrical equipment that protect humans from direct contact with electricity. Around three decades ago, scientists found that by undergoing a structural modification process known as doping, a form of conjugated polymer known as "polyacetylene" could become extremely electrically conductive [4]. Therefore, since the observation of metallic conductivities for iodine doped polyacetylene, [5,6] the perception that “plastics” cannot conduct electricity was broken. Because of the alternating single and double bonds in the polymer chain, the polymer is known as a "conjugated polymer. "Followed by the polyacetylene, the second generation conjugated polymers, such as poly-3 hexylthiophene and poly(para-phenylenevinylene) derivatives, utilize alkyl or alkoxy side chain substituted aromatic rings as the building blocks to construct conjugated polymers, which exhibit good solubility and stability [7]. Consequently, the third-generation conjugated polymers with electron- deficient (accepter)-electron-rich (donor) alternating structures provide more opportunities for polymer design strategies. Among them, much attention has focused on the development of copolymers based on the alternation of accepter–donor units [8,9]. In conjugated polymers, the de-localized electrons excited from HOMO to LUMO can flow across the system and become charge carriers, making it conductive. When electrons are removed from the backbone, which corresponds to oxidation, the molecule become a radical-cation, resulting in a net positive charge, so this polymer is converted into a conducting form. Similarly, electrons can be added to form a radical anion, which corresponds to reduction, and this process makes the

polymer conductive as well, if the polymer structure is suitable. Electrons and holes (negative and positive polarons) operate as charge carriers, jumping from one location to another in response to an electrical field, improving conductivity. The localized form is also called a positive polaron or negative polaron for radical cation or radical anion, respectively. The doping technique is widely acknowledged to be an efficient means of increasing the concentration of charge carriers in dopped materials. Therefore, charge carriers are able to flow. The electrons in the conjugated system, which are weakly bonded, are able to move throughout the polymer chain when doping occurs. The optoelectronic characteristics of conjugated polymers are governed by their electronic coupling, which is closely associated with the conformation of the polymer backbones. Generally, the backbone of conjugated polymers is composed of interconnected carbon atoms with sp^2 hybridization. The remaining parallel p_z atomic orbitals create π molecular orbitals along the polymer chains, and π-electrons play a major role in facilitating charge transfer in conjugated polymers. Charge transfer in conjugated polymers consists primarily of two components: intrachain and interchain charge transport. The intrachain charge transport is directly influenced by the overlapping of π-orbitals along the polymer backbone. In an ideal scenario, the π-orbitals along the backbone will exhibit highly dispersive waves, and their strong electronic coupling can contribute to exceptional one-dimensional charge transport [10]. Moreover, the extensive planar arrangement of the coplanar backbone of the polymer chain engenders robust π-orbital interactions among adjacent chains. These interactions hold significant implications for facilitating the efficient transfer of charges between different chains, underscoring the pivotal role of a rigid coplanar backbone in the charge transport dynamics of conjugated polymers. However, the attainment of such a rigid and coplanar conformation within conjugated polymers proves to be a formidable challenge. In conventional conjugated polymers, aromatic rings are typically connected by single bonds, a structural feature that inherently allows energetically favorable conformation of the backbone which is not coplanar. Considerable strategies have been developed based on molecular design in order to enhance the rigidity and coplanarity of conjugated polymers. **Chyba! Nenalezen zdroj odkazů.** illustrates conventional a nd rigid coplanar conjugated polymers. The planar conformation is locked by interaction of the side groups.

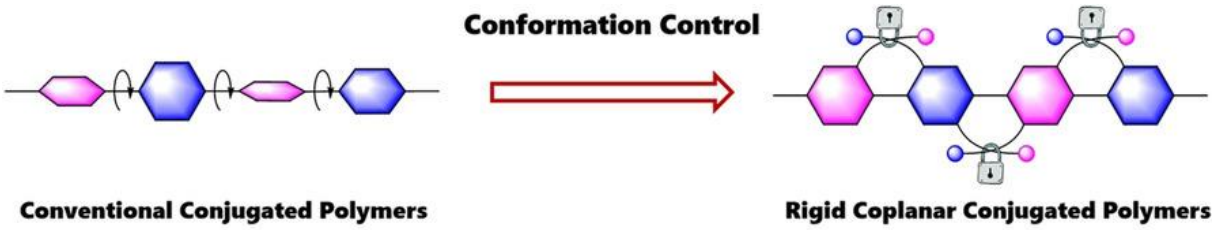

Figure 1 Schematic of a) conventional conjugated polymers b) rigid coplanar conformation, based on [11]. *Note, the circular arrows in the left part of the scheme indicate dihedral angles.*

In recent decades, extensive research has been conducted on the manipulation of the conformation of conjugated polymers. However, within this realm, there remain two areas that have received relatively less attention: firstly, the transition from controlling molecular conformations to understanding how these conformations affect the aggregation behaviours of polymers, and secondly, elucidating how these aggregation behaviours, in turn, impact the macroscopic electrical properties of the materials. Consequently, comprehending the aggregation behaviours of conjugated polymers emerges as a crucial stepping stone towards establishing a robust structure-property relationship [11].

1.2 H- and J-Aggregation

Variations in deposition conditions, such as solvent or temperature, allow for varied packing structures in homopolymer films and varying degrees of phase separation in blend films. Polymer packing structures are likely to influence molecular optical properties, particularly the formation of interchain species such as aggregation and excimer states. Furthermore, a variety of structural characteristics might influence the optoelectronic and charge transport capabilities of conjugated polymer thin films. The orientation of the polymer chains in a device structure with regard to the electrodes, as well as the degree of crystallinity, can have a significant impact on charge carriers' mobility. The rate of interchain charge transfer may be affected by the interchain π-spacing. The torsion angle between neighbouring interchain charge transfer units within a single polymer chain affects the chain's planarity and effective conjugation length, and interchain polymer packing structures can have a major impact on both charge and energy transport [12]. Therefore, a proper understanding of the intermolecular (excitonic) coupling and electron-vibrational coupling concepts leads us to understand the charge and energy transport in soft organic assemblies. The electronic interactions that occur either within a given chain or between chains stem from the aggregates of the conjugated polymer. J-aggregates (H-

aggregates). Aggregation is identified by shifts in photoluminescence energy, changes in vibronic peak ratio, and photoluminescence lifetime [13]. The theoretical framework delineating coherent coupling mechanisms in Conjugated Polymers (CP) was advanced by Spano et al., incorporating a hybrid of J-type and H-type couplings. This framework contrasts conventional J-aggregation occurring in van der Waals-bound aggregates by emphasizing unconventional J-type coupling amid covalently linked repeat units within a polymer chain. Simultaneously, conventional H-type coupling is highlighted between cofacial chromophoric units on adjacent chains, adhering to Kasha's exciton theory [14–16]. J-type coupling predominantly manifests within the same CP chain due to covalent interactions between head-to-tail arranged transition dipole moments (TDMs) of repeat units [17,18]. Increased coupling strength or coupling of additional repeat units, such as through chain planarization, enhancing π-conjugation, results in heightened J-type photoluminescence (PL).

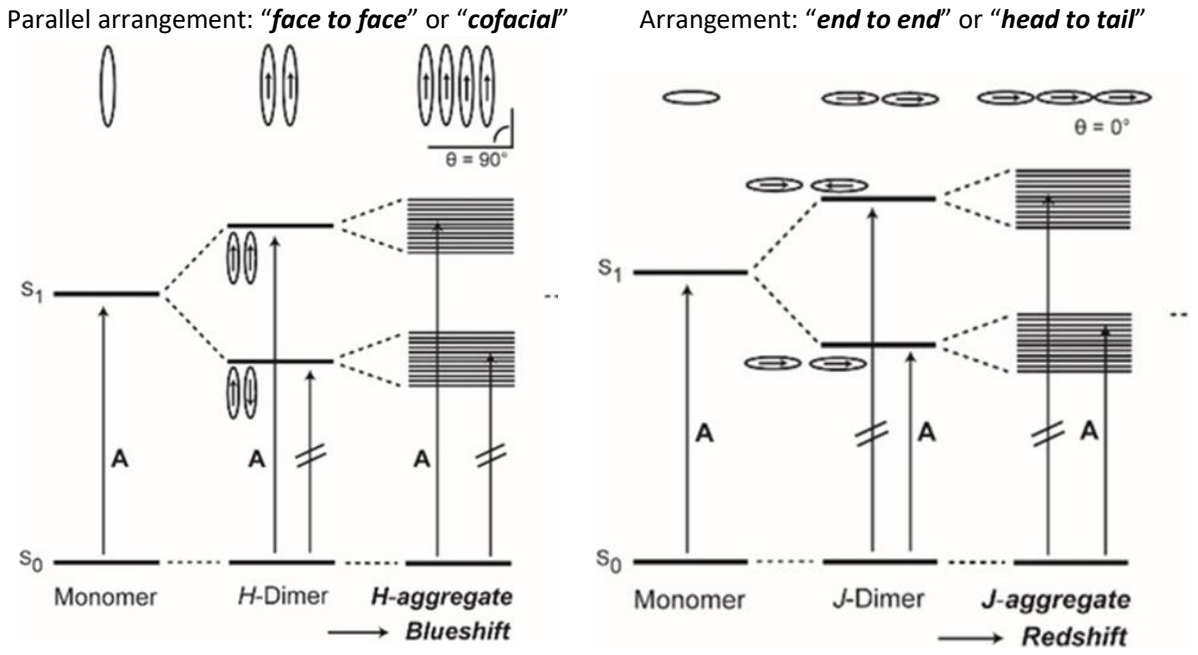

Figure 2 Schematic representation of the photophysical absorption properties of a J- or H- aggregate [19]

Spectroscopically, J-aggregation in van der Waals-bound structures aligns with improved conjugation in covalently bound polymer repeat units [20,21]. Generally, conjugated polymers approximate direct-gap semiconductors, exhibiting positive effective exciton band curvature around $k = 0$, a prerequisite for J-type photophysics [22]. The transition from the lowest excited state to the ground state in a J-type coupled system is dipole-allowed, leading to distinctive

spectroscopic changes in PL compared to an uncoupled system. These changes include an increased radiative rate, reduced PL lifetime, spectral redshift, and narrowing of the 0–0 vibronic transition, along with an increased 0–0 to 0–1 vibronic peak ratio [17] [23,24]. The two aggregate types are depicted in Figure 2. Slipped facial aggregates are tilted aggregates. In this case it depends on the staggering angle as to which aggregation type is formed. A notable exemplar of J-type behavior in CPs is the trans-polydiacetylene isolated chain, demonstrating an effective ratio of 0–0 to 0–1 PL peaks of almost one hundred, indicative of excitonic delocalization of order 100 nm as a result of J-type coupling [19,21,25]. In contrast, H-type coupling primarily occurs between chromophoric units on different CP chains, necessitating a side-by-side arrangement. The transition from the lowest excited state to the ground state in H-type coupling is, in principle, dipole forbidden, resulting in contrasting changes in PL compared to J-type coupling [26–30]. Recognizing these two aggregate types using the usual spectral shifts, on the other hand, might be misleading, especially when evaluating the photophysical response in more complicated morphologies. For example, lutein diacetate aggregates, which were previously thought to be J-like based on spectrum shifts, are really H-like, with absorption ratio - Rabs decreasing considerably with aggregation. Furthermore, despite its H-aggregate structure, an enhancement in intrachain planarization causes a considerable redshift in the case of poly(3 hexylthiophene) (P3HT) [20].

1.3 Nanocomposite

Nanocomposites refer to composite materials wherein one of the phases exhibits nanoscale morphology, such as nanoparticles, nanotubes, or lamellar nanostructures. These materials possess multiple phases, rendering them multiphasic, with at least one phase having dimensions ranging from 10 to 100 nanometres. Nanocomposites have emerged as a strategic solution to address limitations in various engineering materials. Classification of nanocomposites is based on the materials constituting the dispersed matrix and dispersed phase [31]. The rapidly advancing field of nanocomposites enables the synthesis of innovative materials with unique properties. The properties of these materials not only depend on their original constituents but are also significantly influenced by their interfacial and morphological characteristics. They can be formed by blending inorganic nanoclusters, fullerenes, clays, metals, oxides, or semiconductors with organic polymers or compounds. It is noteworthy that the resulting material may exhibit properties unknown in the parent constituents

[32,33] Therefore, the conceptual framework of nanocomposites involves utilizing nanoscale building blocks to design and fabricate materials with unprecedented flexibility and enhanced physical properties[34].

1.4 Nanocomposite polymer thin films

The utilization of polymers in various applications is extensive, owing to their inherent properties; however, their thermal, mechanical, and electrical characteristics often pale in comparison to metals and ceramics. In response, polymer nanocomposites have emerged as a new class of materials, offering a novel approach to augmenting polymer performance. By embedding inorganic nanoparticles within an organic polymer matrix, these nanocomposites introduce enhanced functionality and versatility. Their potential applications extend across various fields, from food packaging to the fabrication of drinkable water bottles, proving their transformative impact. The composition of polymer matrices, ranging from homopolymers to copolymers and blends, underscores the adaptability of this technology. Furthermore, the incorporation of various nanofillers, such as metal oxides and carbon nanotubes, enables precise tuning of properties such as electrical conductivity, magnetic, mechanical, thermal and flame resistance. The good and homogeneous dispersion of nanofillers within the polymer matrix holds utmost significance, as it fundamentally defines the resulting physico-chemical properties of the nanocomposites [35–37].

Several methodologies of polymer nanocomposite preparation stand prominent, each tailored to meet specific requisites. Among these, in situ polymerization emerges as a sophisticated approach, facilitating the simultaneous synthesis of the polymer matrix alongside nanoparticle integration. This technique offers precise control over morphology and particle dimensions, ensuring advanced engineering of material properties. Conversely, melt extrusion, renowned for its versatility and industrial applicability, represents a cornerstone process in polymer nanocomposite fabrication. Operating without solvents, it alters the physical properties of raw materials by extruding them through a die under controlled pressure and temperature conditions. On the other hand, solution dispersion presents an efficient methodology wherein nanoparticles are dispersed within a polymer solution, and subsequent solvent removal yields the desired nanocomposite, making this method ideal for large-scale applications. It is worth pointing out that the solvents utilized in solution dispersion to prepare polymer nanocomposites contain a range of options, including chloroform, toluene, alcohol, acetone, and water. The selection of these solvents depends upon their

compatibility with the polymer and nanoparticles employed in the nanocomposite synthesis process. Factors influencing solvent choices cover considerations such as toxicity levels, solubility characteristics of the polymer, and the desired properties of the final nanocomposite material. Preference often leans towards less toxic solvents like alcohol, acetone, chloroform, and water due to their favorable attributes. Furthermore, the choice of solvent plays a pivotal role in impacting the dispersion and interaction dynamics between nanoparticles and the polymer matrix, thereby influencing the overall dispersion quality and incorporation of nanoparticles within the composite structure. Each of these methodologies offers distinct advantages, catering to diverse needs in producing polymer nanocomposites [38–40].

The method that is used for preparing nanocomposite in this dissertation is solution dispersion or solution mixing because of its abundant advantages. Firstly, it stands out as a quick and straightforward method, perfectly suited for any scale of production ranging from laboratory to industrial, thereby ensuring efficiency in manufacturing processes. Secondly, its capability to uniformly disperse nanoparticles within a polymer solution guarantees a homogenous distribution throughout the resulting nanocomposite material, ensuring consistency and reliability in performance. Furthermore, the flexibility offered in solvent selection allows for tailored compatibility between the polymer and nanoparticles, enhancing the overall quality of the composite. Another significant advantage is the precise control over nanoparticle concentration and loading within the polymer matrix empowers researchers to fine-tune material properties to meet specific application requirements. Last but not least, the opportunity for surface modification of nanoparticles before dispersion enhances their compatibility and interaction with the polymer matrix, ultimately augmenting overall performance [41].

2. Polymer LEDs

There are mainly two kinds of organic light emitting diodes (OLEDs) based on small organic molecules and conducting polymers. It was first introduced by a team in Kodak in 1987 and after few years in 1990, Friend and Burroughes developed polymer light emitting diodes (PLEDs) based on PPV through spin coating technique [42]. Considering that PLEDs are compatible for solution methods, they have great potential to develop large area light-emitting displays. In 1992, Heeger and co-workers successfully prepared PLEDs on a flexible substrate (polyethylene terephthalate, PET), making it possible to create flexible display devices [43]. In 1994, Kido and Matsumoto realized white light-emitting polymer electroluminescent devices with power efficiency of 0.83 lmW^{-1} [44]. PLEDs had several concerns in the early days, including low efficiency and instability. PLEDs, on the other hand, have achieved significant advances and exhibited extensive application possibilities in the areas of display and lighting sources due to the rapid development of electroluminescent materials and device structures. PLEDs have several benefits over inorganic light-emitting diodes, including many applicable materials, low processing cost, compatibility with solution methods, adaptability for large-area manufacturing, and great flexibility [45].

2.1 Structure and Mechanism:

Figure 3 depicts the structure and mechanism of PLED. When a bias voltage is supplied across the device, holes and electrons pass through the interface barrier and are injected into the organic layer from the anode and cathode.

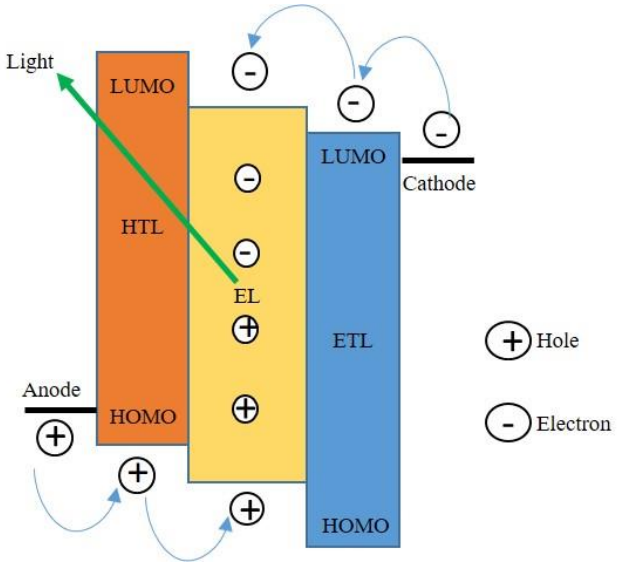

Figure 3 Schematic illustration to the working mechanism of a typical PLED

They transfer into the hole transporting layer's (HTL) HOMO and the electron transporting layer's (ETL) LUMO, respectively. The charge carriers are then stimulated by the external electric field and moved to the emission layer, where they recombine to produce excitons. These excitons are excited and hence unstable. Finally, the excitons transition from the excited to the ground states, resulting in light emission. The energy differential between the LUMO and HOMO of the emitting organic material determines the colour of the light. Thus, by changing the active organic components, the emission colour may be adjusted over the whole visible spectrum [46].

2.2 Substrate and electrodes

OLED substrates are often comprised of plastic or glass. In order to boost hole injection in HTL, the anode material should have a high work function. The most common anode material is indium tin oxide (ITO), which has a high work function. It is also transparent. A low work function is required for the cathode to allow electron injection in ETL. Cathode materials are often magnesium silver alloy, barium, and aluminium.

2.3 Performance

Conjugated polymer is sandwiched between the cathode and anode in single-layered PLEDs. Because of its simplicity and ease of fabrication, this single-layer structure is common. However, the light-emitting material must have both high quantum efficiency and relatively equal electron and hole mobility; otherwise, an imbalanced injection of electrons and holes would occur, reducing device efficiency. The electron blocking layer, hole injection layer, hole transporting layer, electron transporting layer, electron injection layer, and hole blocking layer are all introduced in a multi-layered structure to provide effective and balanced charge carrier injection. A charge injection layer is used to reduce the barrier between the electrode and the charge carrier transporting layer, thereby increasing the number of injected charge carriers; a charge blocking layer is used to confine most of the charge carriers to the emission layer, enhancing quantum efficiency.

3. AIM OF THE THESIS

The aim of this study is to examine the correlation between the structure of conductive polymers in thin films and their optoelectronic and electrical characteristics. Additionally, the research aims to explore a specific modification technique that involves the introduction of non-conductive nanofiller to a polymer matrix in order to attain explicit optical and electrical properties. The accomplishment of the aim may be outlined in the following goals and objectives:

- Neat polymer thin film preparation and characterization

To achieve the aim of this investigation, thin films derived from pristine polymers F8BT and MEH-PPV will be prepared. The study will focus on the dependence of structural (dis)ordering on the thickness in the case of F8BT thin films, and consequently its potential impacts on optical and electrical properties of the thin films. Thin films from neat MEH-PPV will be prepared as a reference, as their thickness depended properties have been reported earlier by other members of the team [47].

- Nanocomposite preparation

Nanocomposite materials containing non-conductive fillers will be prepared. The investigation will examine the correlation between the changes in the structural (dis)ordering of the conjugated polymer imparted by the nanofiller and how these changes are manifest in the ultimate properties of the nanocomposites. The thin films will be made from the well-known standard study material MEH-PPV and concentration of the added non-conductive filler Al_2O_3 nanowires will be varied. The shape of the filler was chosen as having potential to impart larger disorder than a simple spherical shape.

- Study of the effects of nanofillers' on the performance of the prepared LED devices

To describe how the addition of nanoparticles influences the properties in final devices, it will be needed to prepare PLEDs comparable with neat polymer standards. All other conditions will be kept the same. The performance of prepared Meh-PPV/Al_2O_3 nanocomposite diodes will be studied, and the obtained results will be interpreted.

4. EXPERIMENTAL

Standard experimental spectroscopic characterization methods were used throughout this work. The background of the less known ER-EIS method is explained in the publication [BG] and references therein. The specific preparation of examined materials and samples is provided here briefly.

4.1.1 Thin film preparation

4.1.1.1 F8BT thin films

In order to achieve thin films spanning thicknesses ranging from tens to hundreds of nanometers in the experiments detailed in this thesis, solutions containing polymer F8BT in toluene (100 µl) were deposited onto quartz glass and ITO-coated quartz glass substrates via spin coating. To prevent the impact of oxygen and moisture on the samples, all solutions and thin films were fabricated within a glovebox environment. Films exceeding 200 nm in thickness were achieved by casting F8BT solutions with concentrations of 1.5% and 3.0% onto prepared quartz and Indium Tin Oxide (ITO) coated quartz substrates.

4.1.1.2 MEH-PPV/Al2O3 nanocomposite and thin films

Nanocomposite thin films were fabricated by initially dissolving MEH-PPV poly [2 - methoxy- 5- (2- ethylhexyloxy)- 1,4 phenylenevinylene] (Mw: 40,000 - 70,000 g mol^{-1}) in chloroform at a concentration of 10 mg/ml, mixed solutions were prepared by incorporating the appropriate quantity of Al_2O_3 nanowires to MEH-PPV solutions. Prior to casting, the dispersions of nanoparticles in the polymer solution underwent sonication. Subsequently, the thin films were deposited using a spin coater on indium tin oxide (ITO) and quartz glass (QG) substrates in the glove-box to protect the films against oxygen.

4.1.2 Preparation of functional devices

The PLED devices featuring a composite active layer of polymer/Al_2O_3 were fabricated within an inert (N_2) atmosphere on patterned ITO substrates containing six active pixels. PEDOT: PSS was deposited as the HTL (hole transporting layer) using standard procedures. A solution containing polymer/Al_2O_3 in chloroform was applied onto the HTL layer through spin coating. Subsequently, the coated layer was dried at 150 °C for 30 minutes. The resulting active layer thickness in the device measured 45 nm. Finally, a magnesium cathode was deposited via sputtering. All PLED devices underwent encapsulation in an epoxy resin before being removed from the protective atmosphere.

5. RESULTS AND DISCUSSIONS

The primary emphasis of the study lies in the experimental preparation and characterization of polymer thin films. Significant progress has been made in various directions outlined by the objectives of the research. This chapter provides a comprehensive summary of the experimental results obtained, beginning with a detailed characterization of the materials and thin films, followed by an examination of the characterization of PLED devices. Furthermore, the results are discussed along with their presentation to ensure that the reader maintains context throughout.

5.1 Study of F8BT thin films with different thickness

5.1.1 UV-VIS Spectroscopy

Figure 4, illustrating the contrast between the spectra of films and the thinnest film (10 nm), provides a clearer depiction of the variations and order development.

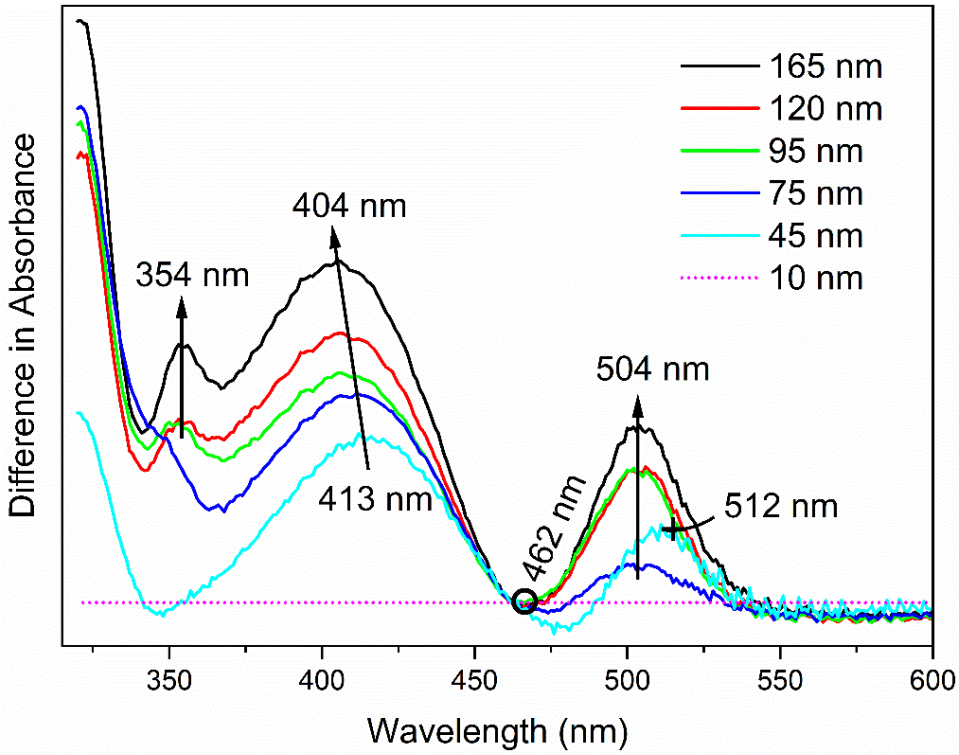

Figure 4 Difference between the spectra for thin films and the spectrum of the thinnest one. Magenta dot line indicates zero difference for the 10 nm sample itself [BG].

The reference point, represented by an empty circle, corresponds to the absorbance at the maximum wavelength for a 10 nm film and was utilized to

normalize the spectra. Additionally, a peak centered a 504 nm was observed, indicating broadening of the absorption peak in the original spectra. The only exception is the 45 nm thick film, which demonstrates maximum broadening at 512 nm. The negative valleys to the right of the reference point prominently demonstrate a blue shift of the maxima for films 45 nm and 75 nm thick. However, for other films, the broadening effect predominates over the blue shift. Notably, the maximum broadening on the blue side of the absorption peak intensifies from 413 nm to 404 nm. Additionally, a distinct feature emerges at 354 nm, which is not discernible in thinner films. These alterations could be ascribed to the formation of a new energy state arising from interchain aggregation states between polymer chains [48]. Nevertheless, if the preference for the formation of H-aggregates is more pronounced in thicker films, the absorption spectra would tend to broaden towards longer wavelengths. However, this contradiction can be elucidated by considering the formation of JH-aggregates, where the interaction between these two aggregation modes results in broadening towards higher energies. This concept aligns with Donley's suggestion in[48], where it was termed as "polymer chain alternating-stacking".

5.1.2 (PL) Spectroscopy

In Figure 5, representative room temperature photoluminescence (PL) spectra of F8BT films are depicted. The excitation spectra (left side) illustrate that the positions of excitation maxima and the overall shape of the spectra are influenced by film thickness. As the thickness increases from 45 nm to 120 nm, a minor blue shift and significant broadening of these peaks are observed. Notably, in the thickest film, a substantial change in spectral shape and a redshift of excitation maxima were detected. These phenomena can be attributed to the extension of the conjugation length along the polymer chain. The increase in the length of conjugated segments results in higher delocalization of excitons, leading to a greater shift of excitation maxima towards lower energy levels of transition vibrational states [49]. In the right graph, the 0-0 peak (representing exciton recombination from the 0^{th} vibrionic excited state to the 0^{th} vibrionic ground state) shows a slight red shift with increasing thickness. Moreover, as the thickness increases, there is a significant increase in the spectral intensity of the second peak (denoted as 0-1, representing exciton recombination from the 0^{th} vibrionic excited state to the 1^{st} vibrionic ground state). In the thinnest film, the 0-0 PL transition is observed at 537 nm. Successively, the emission maxima of the 0-0 transition shift towards 545 nm for films ranging from 45 nm to 200 nm in thickness. However, when the film thickness exceeds 200 nm, the 0-0 transitions nearly vanish from

the spectrum, and the 0-1 transition becomes predominant. This shift in the 0-0 transition can be attributed to a modification in polymer chain packing [48], where J-aggregation of chains facilitates this transition. Indeed, with increasing thickness, the polymer chains tend to form a more ordered film, favoring H-aggregation with alternating stacking of polymer chains, consequently altering the spectral properties of the material. The structural ordering of chains leads to the dominance of the 0-1 transition with a longer conjugation length in the thickest films, resulting in low-energy radiative states [48][50].

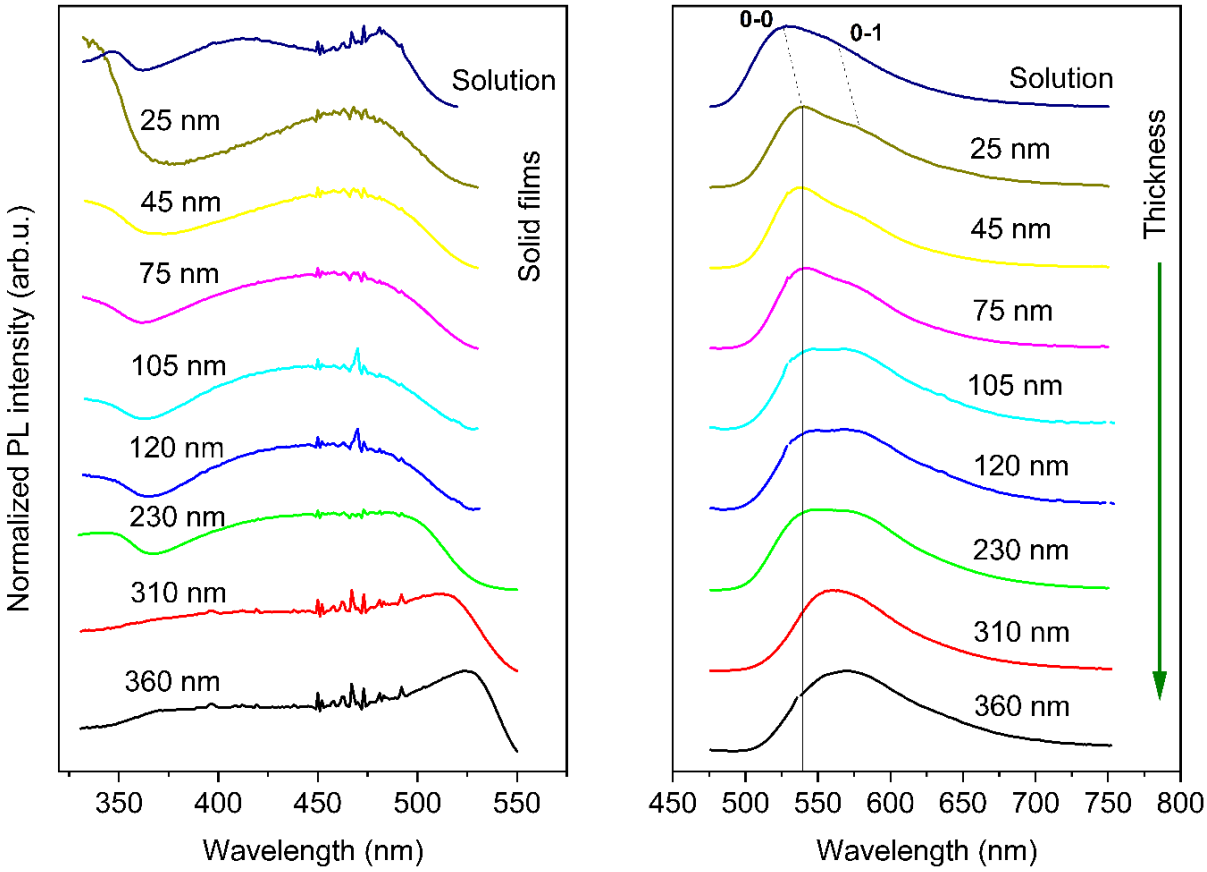

Figure 5 Excitation (left), λ_{em} = 576 nm and emission (right), λ_{ex} = 466 nm spectra of F8BT solution and films with different thicknesses [BG].

5.1.3 ER-EIS

In the band gap region (light grey area I), the Density of States (DOS) noticeably diminishes with increasing film thickness. The reduction in DOS as a function of film thickness. This phenomenon can be attributed to a general enhancement in polymer chain structural ordering and the formation of ordered units, leading to a decreased population of defect states within the gap. [50]. Another noteworthy feature observed in the grey area II (Figure 6) s the existence of shallow states positioned 0.5 eV below the LUMO (-2.65 eV) in the thinner

polymer films. The presence of shallow states is likely attributed to the introduction of disorder in polymer chain packing, which can disrupt the alternating structure of adjacent BT and F8 mer units in neighboring polymer chains [51]. Such a structural characteristic is expected to enhance interchain electron transfer (hopping) by facilitating the population of states around -3.15 eV.

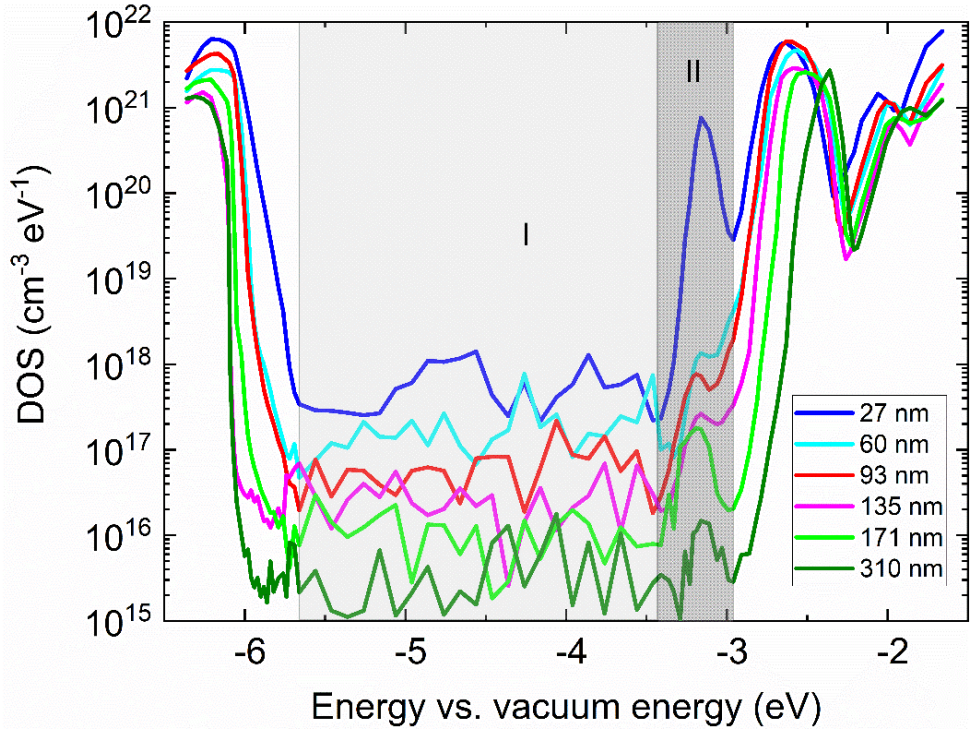

Figure 6 ER-EIS spectra of F8BT films with different thicknesses [BG].

5.2 Study of polymer nanocomposite MEH-PPV/Al_2O_3 thin films

5.2.1 UV-VIS spectroscopy

We analyzed the optical band edges and the optical gap of the polymer in solid thin film form using Tauc's plot and Urbach's tail analysis of the UV/vis absorption spectrum, depicted in Figure 7). The primary absorption band is centered around the maximum at 499 nm (2.48 eV). The transitions within this region (referred to as T1) correspond to π–π* electron transitions along the main polymer chain. Additionally, the region T2 signifies electronic transitions originating from localized and delocalized electronic levels within the polymer [52]. The introduction of nanoparticles does not alter the transition structure in the T1 region, and the maxima remain unshifted. However, the impact of nanofillers

is evident through the extended absorption observed in the tail region, which can be further divided into the weak absorption transition region (WAT) and the Urbach region (U). As nanoparticles are increasingly incorporated, the absorption in the Weak Absorption Transition (WAT) region rises. This can be ascribed to the emergence of new states linked to structural disorder within the polymer matrix induced by the addition of nanofillers[53].

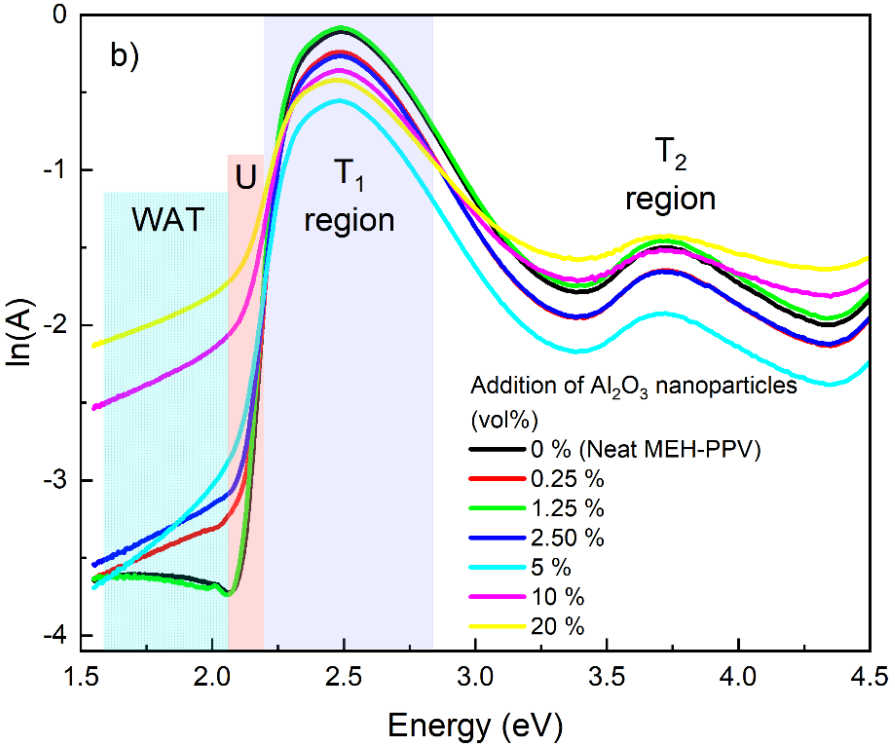

Figure 7 Absorption spectra of prepared thin films analyzed in agreement with Urbach's theory.

5.2.2 (PL) Spectroscopy

The emission spectrum of neat MEH-PPV comprises two main peaks. The first peak, at 2.11 eV (587 nm) is characteristic of emission from the backbone chain, arising from the relaxation of excited π-electrons from the 0^{th} vibrational level in excited state to the 0^{th} vibrational ground state level (0-0), Meanwhile, the peak at 1.96 eV (633 nm) is associated with interchain interaction states [54] and it is attributed to the relaxation from the 0^{th} vibrational excited state to the 1^{st} vibrational ground state level (0-1) [55]. Significant changes related to the amount of nanofiller are evident in the emission spectra, as depicted in Figure 8.

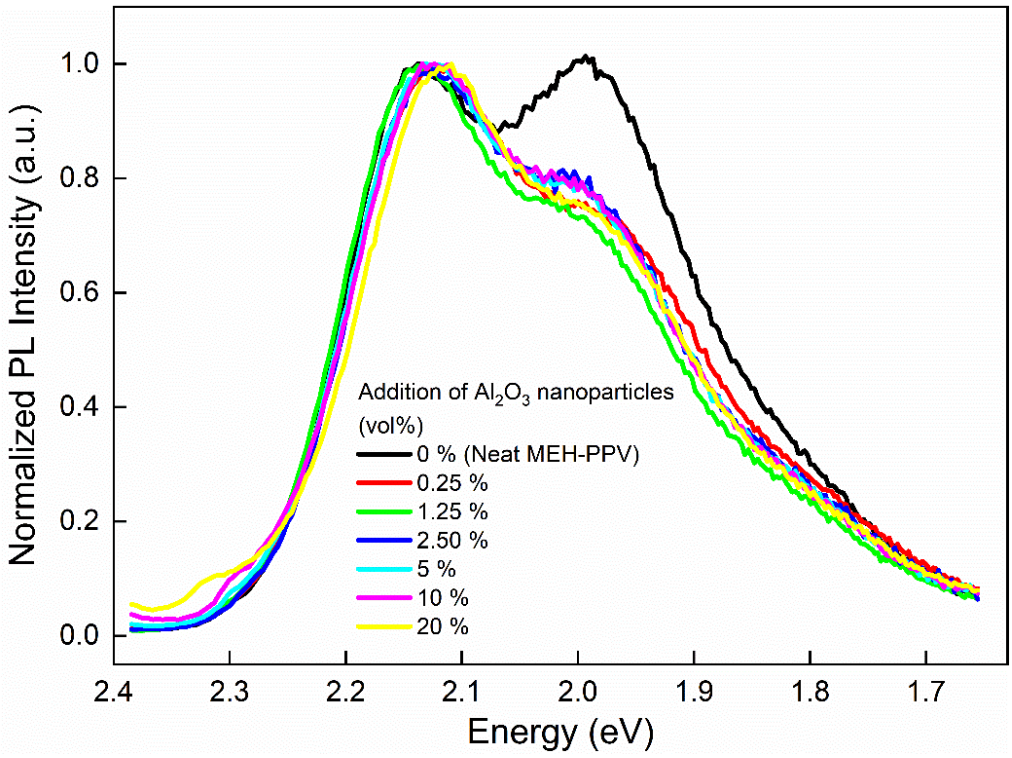

Figure 8 Normalized photoluminescence emission spectra of prepared MEH-PPV thin films on ITO substrate

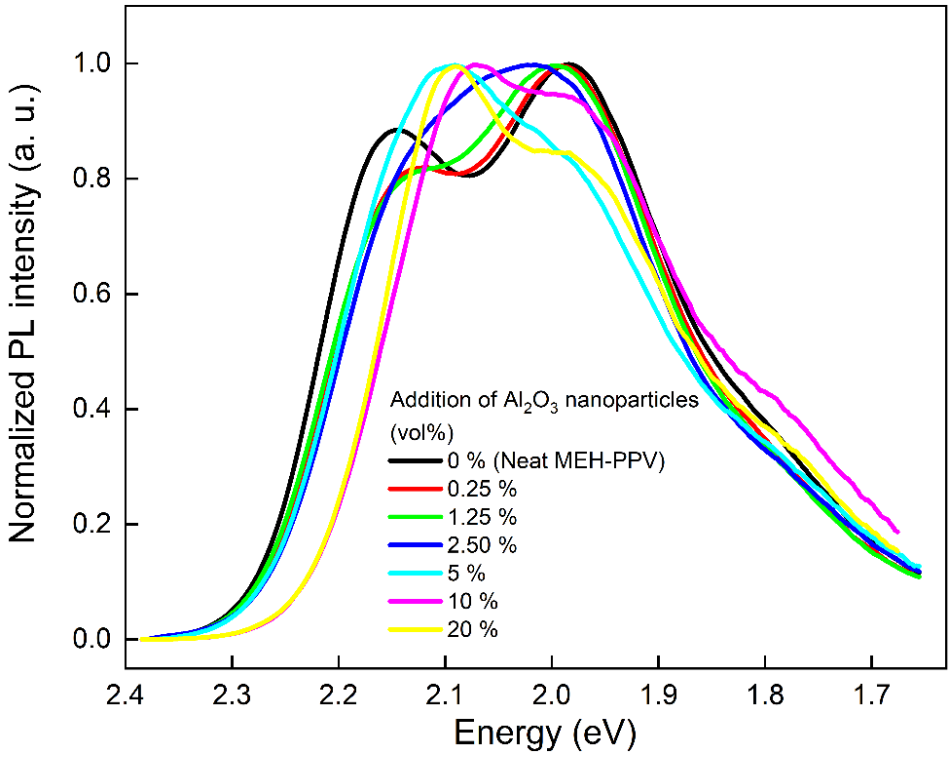

Figure 9 Normalized photoluminescence emission spectra of prepared MEH-PPV thin films on QG substrate

The inclusion of nanofillers impacts the intensity ratio of the 0-0 and 0-1 exciton radiative recombination transitions. In the case of layers with a thickness of 100 nm, neat MEH-PPV exhibits a predominance of the 0-1 recombination channel, indicative of layers with a better-organized structure, as previously demonstrated and discussed[55][56]. Conversely, the addition of nanoparticles induces a shift in the ratio of radiative events in favor of the 0-0 channel. As the amount of nanofiller increases, the intensity of the 0-0 transition compared to the 0-1 transition also increases. The photoluminescence (PL) spectra were measured on thin films deposited on both ITO (Figure 8) and QG (Figure 9) substrates. For films on the ITO substrate, the trend in the evolution of PL peak area ratios (refer to Figure 10) is straightforward, with a slight increase observed. The only minor anomaly is noted in the sample with a filler content of 0.25 vol %. Conversely, for layers deposited on QG substrates, the trend is somewhat more intricate.

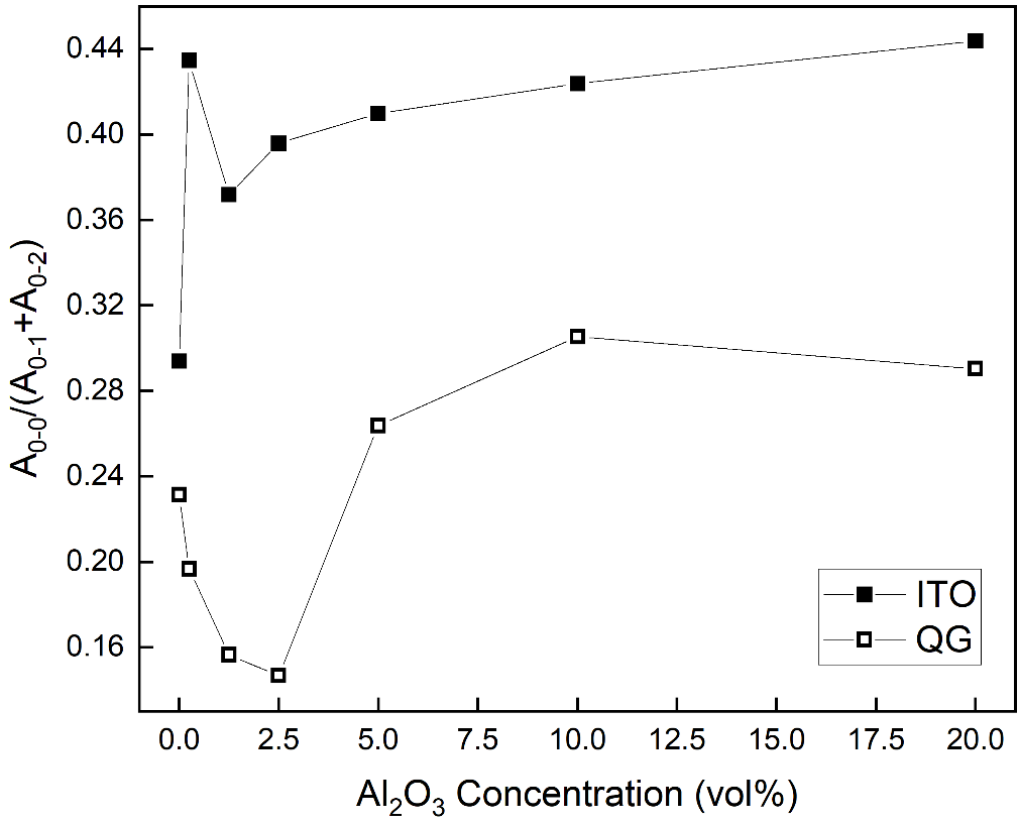

Figure 10 The dependences of the PL peak area ratio on nanoparticles concentration

Given that QG substrates are smoother compared to ITO the filler content is expected to have a significant impact. The peak ratio declines until reaching the nanofiller content of 2.5 vol %, after which it begins to increase. This transition marks a turning point in the development of electronic transitions during radiant

recombination and associated optoelectronic properties. Other studies have also shown the dependence of the polymer layer structure on the layer thickness. [BG][55][49,50]. Maintaining consistency across all these parameters allowed us to isolate the influence of nanofiller addition. It is conceivable that the nanoparticles induce a steric effect, creating distance between the chains and thereby impeding the formation of interchain Coulombic interactions. This disturbance, if not outright prevention, of macromolecular chain stacking may result from the presence of nanoparticles. Consequently, the chains will tend to arrange preferentially in J-aggregated structures, resulting in a state where 0-0 recombination becomes predominant. This explanation aligns perfectly with the theory of J- and H-aggregates and with the elucidation of their formation[57][15].

5.2.3 SPV and CELIV

Table 1 presents the values of the determined exciton diffusion lengths. A distinct trend emerges from the provided values, indicating that the exciton diffusion length decreases with increasing filler content. Specifically, the exciton diffusion length decreases from 14 nm (neat MEH-PPV) to 1 nm (sample with 5 vol % or 10 vol % filler). The photovoltaic effect hinges on the presence of an electric field for the dissociation of photogenerated excitons. This field is established within the space charge region (SCR) at the ITO/polymer interface. Upon illumination, excitons are generated both within the neutral bulk and within the SCR. Excitons diffusing within the bulk contribute to a diffusing current, while a drift current arises from excitons generated within the SCR. The total photocurrent is the aggregate of both contributions [58].

Table 1 Values of exciton diffusion length (L) and charge carrier mobility (μ).

Samples	L (nm)	μ (cm^2/Vs)
Neat MEH-PPV	14	1.8×10^{-5}
0.25 V%	15	1.1×10^{-5}
1.25 V%	14	-
2.50 V%	10	1.4×10^{-5}
5 V%	2	1.6×10^{-6}
10 V%	1	-
20 V%	-	-

The reduction in the diffusion length observed in samples with increasing nanoparticle concentration likely stems from heightened structural disorder and

an augmented density of states within the band gap. For nanoparticle concentrations exceeding 10 vol %, the diffusion length becomes exceedingly small, leading to the photogenerated current primarily originating from the space charge region (SCR). However, an alternative mechanism of photogenerated charge collection exists, which is independent of the diffusion length. The hole mobility μ in both neat MEH-PPV and MEH-PPV with various concentrations of Al_2O_3 nanowires was investigated using the CELIV method. The resulting values have been included in Table 1. For samples with $L \geq 10$ nm, the mobility ranges from (1.1 to 1.8) × 10^{-5} cm^2/Vs and is roughly correlated with the diffusion length. However, in the sample with L = 2 nm, the mobility is one order of magnitude lower. This discrepancy may be attributed to the addition of nanoparticles, where a concentration of at least 5 vol % introduces a significant increase in disorder within the film structure, impacting the transport of charges in the matrix and subsequently reducing the mobility of holes. In samples with a filler concentration exceeding 10 vol %, the diffusion length of excitons is likely no more than 1 nm, given the observed decrease in diffusion length with this concentration. However, we approach the estimation of exciton diffusion length with caution and thus refrained from providing specific values for the most filled samples. Furthermore, the decline in charge carrier mobility correlates with the reduction in exciton diffusion length.

5.2.4 ER-EIS

The ER-EIS method was employed to intricately map the band structure of thin MEH-PPV nanocomposite layers. The density of states (DOS) spectra for neat MEH-PPV and thin films with varying concentrations of nanofiller are presented in Figure 11 depicted on a logarithmic scale. The analysis reveals that the presence of filler alone does not alter the distribution of states within the band gap. However, an observable trend emerges: as the concentration of nanofiller within the matrix increases, there is a corresponding rise in the number of defect states within the band gap of MEH-PPV. The defect states concentration exhibits a notable increase beyond the 5 vol % concentration threshold. This observation aligns with the increased disorder detected through GIWAXS analysis in the MEH-PPV films containing incorporated nanoparticles. It suggests that the heightened defect states induced by the addition of nanofiller are a consequence of the structural disorder introduced into the MEH-PPV film.

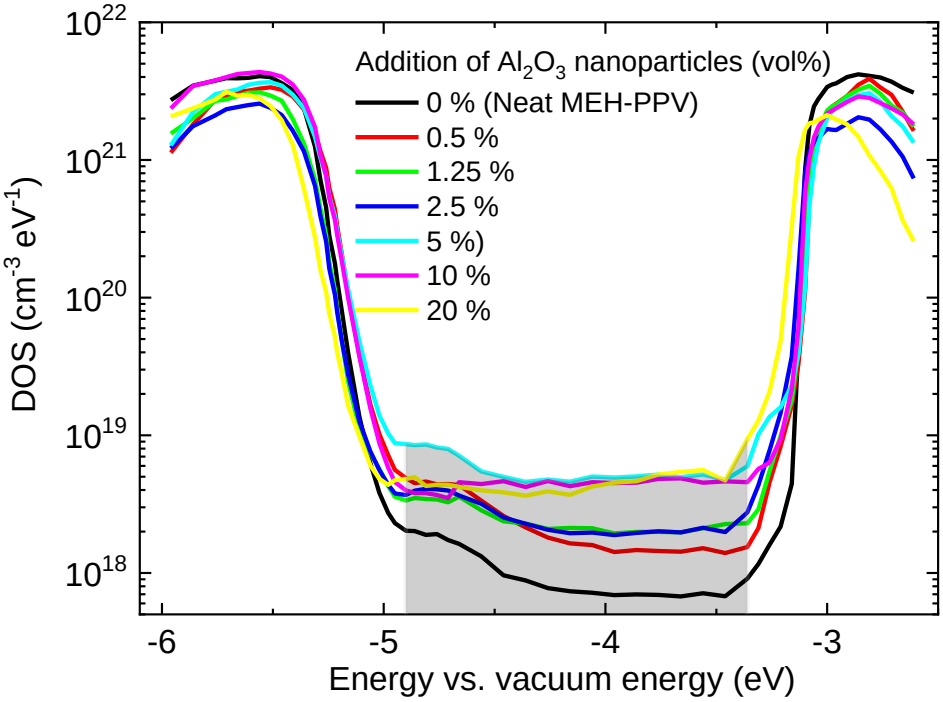

Figure 11 The representative ER-EIS spectra of prepared thin films with different amount of nanofiller in logarithmic scale.

5.3 Study of nanocomposite MEH-PPV/Al_2O_3 LEDs

In our study, we extended the investigation to the practical application of light-emitting diodes (LEDs) to showcase the beneficial impact of the nanofiller. Here, nanocomposite materials MEH-PPV/Al_2O_3 were utilized as the active light-emitting layer.

As it is shown in Table 2, the luminance values decline gradually, starting from 220 Cd/m^2 for neat MEH-PPV to levels in the order of tens of Cd/m^2 for varying nanoparticle concentrations. Concurrently, the current efficiency experiences a dramatic decrease post-nanoparticle addition, stabilizing at approximately the same level after the inclusion of 1.25 vol % of nanoparticles. The data further reveal that diodes incorporating an active layer with 0.25 and 1.25 vol % of nanoparticles achieved nearly twice the electrical power. This phenomenon arises from the requirement for the same or lower current to pass through the layers, albeit at a higher voltage. Despite the increase in electrical power, however, a corresponding elevation in luminance was not observed.

Table 2 Comparison of parameters of prepared polymer LEDs operated at the maximal electric power.

Addition of Al_2O_3 (vol %)	Sample	Maximum luminance (Cd/m^2)	Luminance at el. power 0.5 W (Cd/m^2)	Current efficiency (mCd/A)
	Neat MEH-PPV	**220**	**150**	**21.92**
	0.25	**140**	**30**	**9.16**
	1.25	**45**	**22**	**2.29**
	2.5	**20**	**18**	**2.90**
	5	**19**	**15**	**3.62**
	10	**10**	**7.5**	**1.69**
	20	**12**	**10.6**	**2.08**

However, there is an observable enhancement in the stability of electrical power, ensuring a sustained current flow through the device. This phenomenon is depicted in Figure 12. In the case of composites, following an initial surge in voltage (a phenomenon colloquially termed "burning"), the voltage required to sustain this constant current diminishes and subsequently stabilizes or continues to exhibit a slight decline. On the contrary, for neat MEH-PPV, the voltage necessary to uphold a steady current in the device exhibits a persistent rise over time. This trend can be elucidated by the onset of the Poole-Frenkel effect in heavily filled composite layers. As the concentration of defect states within the band gap escalates, trap-assisted electron transport is prolonged, contributing to the observed behavior [59]. Moreover, the intrinsic MEH-PPV polymer is susceptible to chain scission, a phenomenon that diminishes carrier mobility. This reduction in mobility is evidenced by a progressive elevation in the transport barrier within the material, necessitating greater voltage compensation to sustain a consistent current flow[60]. Conversely, in diodes made with a nanocomposite active layer, voltage exhibited an initial surge upon diode activation at the onset of the measurement period. Subsequently, the voltage either stabilized or exhibited a slight decline during subsequent operational intervals. Examples of prepared devices in State On; luminance at electric power 0.5 W is illustrated in Figure 13.

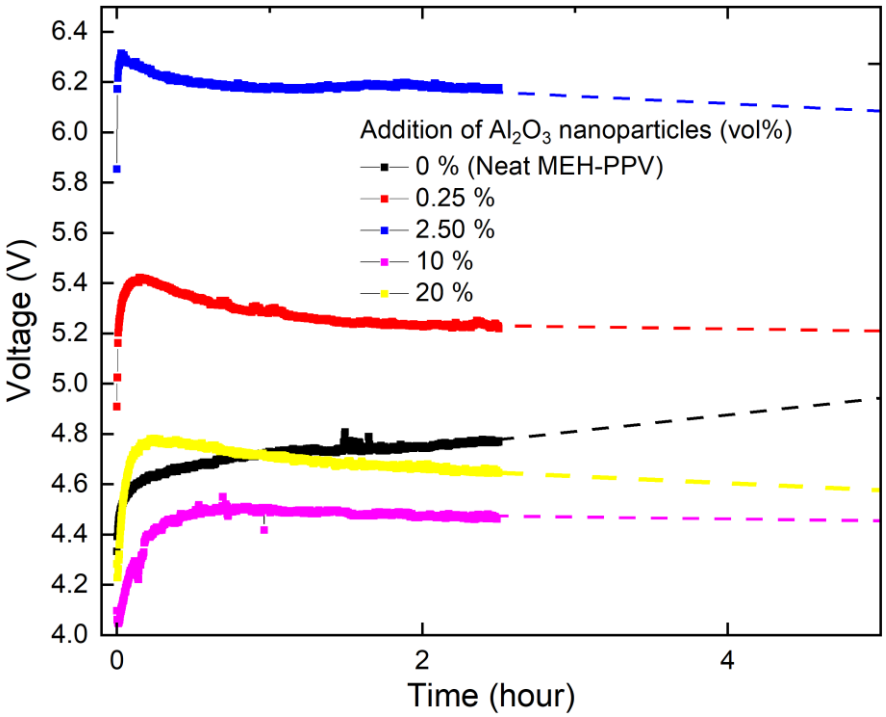

Figure 12 Time dependence of the applied bias voltage maintaining a constant current of 0.1 mA.

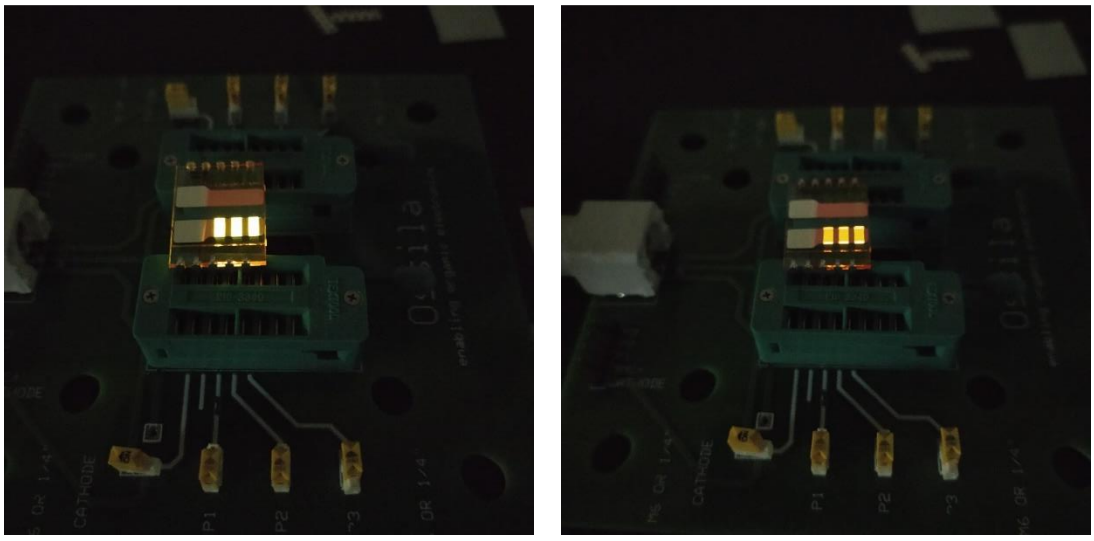

Figure 13 Examples of prepared devices (device on the left side contains MEH-PPV only, the one on the right side contains MEH-PPV with nanofillers).

6. CONCLUSIONS

The aim of this study is to reveal and demonstrate a significant dependence of electronic structure and optoelectronic properties of conducing polymer thin films on their thickness, presenting a non-trivial relationship. Moreover, to examine the impact of non-conductive fillers on the structural ordering of conjugated polymer chains and explore whether modifying the structure of the active layer in an electronic device using nanofillers can lead to specific enhancements in device performance.

Following this concept, to present a comprehensive study of structural ordering impact on the electrical and optoelectronic properties of F8BT, a series of thin films with various thicknesses of the F8BT conjugated polymer was prepared on selected substrates. UV-Vis absorption, photoluminescence spectroscopy (PL), energy resolved-electrochemical impedance spectroscopy (ER-EIS) and grazing-incidence wide-angle X-ray scattering (GIWAXS) were used to investigate the optical and optoelectronic changes of the thin films with increase in thickness.

According to the UV-Vis absorption spectra the main absorption peak, associated with π-π^* electron transitions along the polymer chain, underwent a slight blue shift with increasing thickness, accompanied by a broadening of the absorption band. The observed changes, suggested potential interchain aggregate states between polymer chains, possibly explained by the creation of JH-aggregates. Photoluminescence spectra study revealed thickness-dependent variations in both excitation and emission spectra of polymer films. Increasing film thicknesses (45 nm to 120 nm) leaded to a slight blue shift and pronounced broadening of excitation peaks, while the thickest film exhibited a significant spectrum shape change and redshift of excitation maxima. These observations could be attributed to the extension of conjugation length along the polymer chain, causing higher delocalization of excitons and a shift towards lower energy levels in excited states. In emission spectra, for films thicker than 200 nm, the 0–0 transitions decreased, and the 0–1 transition became dominant, that could be ascribed to changes in polymer chain packing favoring H-aggregation. The deconvolution of emission peaks and the analysis of the ratio of peak areas further supported the transition from J-aggregation in thinner films (below 120 nm) to H-aggregation in thicker films (over 120 nm), influencing the radiative transitions. There was an obvious correlation among the ratio of emission peaks, the presence of a satellite peak in DOS spectra, and the film thickness. The 0–1 transition

increased with growing thickness, indicating a potential reduction in the satellite density of states (DOS) peak below the LUMO. This reduction led to a non-radiative transition instead of the 0–0 transition. The increased transport gap in the case of thicker films was caused by lower structural disorder, which led to coherent charge transport along the main chain which is weaker than hopping in F8BT films. The films were found to contain crystalline phases characterized by both face-on and edge-on orientations of F8BT chains. The shift in electronic structure aligned with the transition from edge-on to face-on phase volume ratio, suggesting a growing prevalence of edge-on orientation in thicker films. The main distinction between films with thicknesses below 100 nm and those exceeding this value lied in the interaction between J- and H-aggregation modes within the film structure. In thinner films, the impact of J-aggregation was prominent, whereas thicker films are characterized by the dominance of H-aggregation. This involved alternating π-stacking of F8 and BT units, promoting enhanced structural ordering.

We noted a critical thickness threshold in various aspects of the films, occurring around 100 nm, marking the boundary between nano- and microscales. Although for each combination of polymer, solvent, and process conditions, a distinct threshold value might be anticipated. However, the approximately 100 nm length scale appears to be a common characteristic of this phenomenon in general. It is worth pointing out that this phenomenon is being addressed for the first time in the context of F8BT, focusing on the packing structure and the formation of H- and J-aggregates. The results of this research were already published [BG].

For the second work we took a more advanced stride in the exploration of the effect of nanofiller (Al_2O_3) in the polymer matrix MEH-PPV Poly[2-methoxy-5-(2-ethylhexyloxy)-1,4-phenylenevinylene] on optical, optoelectronic, and electrical properties. Considering the existence of a thickness threshold at approximately 100 nm, we created two sets of thin films with thicknesses below and around 100 nm. In both sets, the film thickness remained constant, while the nanofiller concentration varied and ITO and QG were used as substrates. First of all, the effect of addition of nanoparticles on optical and optoelectronic properties was investigated using UV-Vis, photoluminescence (PL) and surface photovoltage (SPV) spectroscopy. Charge extraction by linearly increasing voltage (CELIV) and the energy-resolved electrochemical impedance spectroscopy (ER-EIS) were used for the determination of the nanoparticles'

impact on the electrical properties, namely on the mobility of charge carriers and electronic band structure, respectively. Grazing-incidence wide-angle X-ray scattering (GIWAXS) and atomic force microscopy (AFM) determined the microstructural features of prepared composite layers. Secondly, to show the effect of the microstructure and assess the impact of nanofillers from a real-world and applied perspective, we manufactured light-emitting diodes (LEDs) and employed the thinner films as the active layer. It is worth mentioning that commercially available Al_2O_3 nanowires were chosen to be used in our experiment These properties were investigated using UV-Vis absorption, and photoluminescence spectroscopy. Exciton diffusion length was examined using the surface photovoltage (SPV) method, mobility of charge carriers was evaluated with charge extraction by linearly increasing voltage (CELIV) measurements. Information concerning the band structure was obtained using energy resolved-electrochemical impedance spectroscopy (ER-EIS). The influence of nanoparticles on the development of the micro structure in thin layers was examine with grazing-incidence wide-angle X-ray scattering (GIWAXS). Luminance, current efficiency, and stability of prepared polymer light emitting diodes were tested.

UV-VIS spectra exhibited no change in main absorption band on the other hand the creation of new states as nanoparticle concentration increases higher than 2.5 vol % was observed that could be linked to structural disorder in the polymer matrix caused by nanofiller addition. Since fluorimetry provides greater sensitivity in characterizing electronic transitions linked to thin film structure, we opted to measure the photoluminescence spectra of thin films on both ITO and QG substrates. The selection of diverse substrates was intentional, highlighting that changes in optoelectronic properties are influenced not only by the substrate's inherent nature but also by the introduction of nanoparticles that was proved by the changes in the intensity ratio of the 0-0 and 0-1 exciton radiative recombination transitions. Moreover, the results obtained from lifetime measurements showed the influence of nanofiller on the lifetimes below 2.5 vol.% and above 2.5 vol.%. The modified SPV method revealed a clear trend: as filler content increased, the exciton diffusion length decreased from 14 nm to 1 nm. This decline could be attributed to heightened structural disorder and density of states in the band gap.

Furthermore, upon the introduction of nanoparticles into the MEH-PPV polymer matrix, a disruption in the polymer chain order occurs, leading to

discernible consequences such as the appearance of additional defect states within the band gap, a decline in charge mobility, and a shortened exciton diffusion length. Consequently, these alterations contribute to a reduction in the maximum luminance of the fabricated diodes and a decrease in current efficiency. Conversely, the inherent degradation of the polymer is notably decelerated, resulting in an extension of the diode's lifespan. Furthermore, a critical nanoparticle concentration threshold exists for the MEH-PPV/Al_2O_3 system. Beyond 2.5 vol.% of nanoparticles in the MEH-PPV matrix, there are substantial changes in density of states, optoelectronic properties, exciton diffusion length, and charge carrier mobility.

We tried to understand a significant factor affecting the MEH-PPV polymer matrix when employed in light-emitting diodes. In prior studies, my colleagues uncovered the positive impact of semiconductor nanoparticles on the ultimate efficiency of PLED devices[61]. However, it remained unclear whether this enhanced efficiency resulted from the manipulation of the polymer matrix structure or the semiconducting properties of the nanofiller. Through this study, the uncertainty between these two influences was addressed by introducing non-conductive nanoparticles into the polymer matrix. The semiconductor nanoparticles can influence the electroluminescence efficiency positively or negatively, depending on their contribution to the charge carrier transport balance, while inevitably imparting some structural disorder to the polymer matrix as well. The role and effects of the disorder itself were demonstrated for insulating nanoparticles in this study. Such particles can prolong the lifetime of the device even at smallest concentrations, but can also can diminish the luminance of the device, especially at high concentrations.

7. Concluding remarks

7.1 Contribution to Science and Practice

This study makes a modest yet distinctive contribution to the broad field of research on charge transport in semiconducting conjugated polymers. Since the packing structure of polymers, particularly in the solid state, plays a crucial role in determining their optical and electrical properties, in our first work, a number of polymer thin films with different thicknesses were prepared and several techniques were employed to investigate the packing structure of prepared polymer thin films. Our comprehensive investigation led to discovering a thickness threshold for the first time for F8BT polymer where one of the HJ aggregations could become dominant. It is worth mentioning that as we used a pretty accurate, unique, and complicated method to calculate the density of states (DOS) of F8BT thin films, our work plays a crucial role in helping other scientist to describe, prove the authenticity of their results and achieve new findings. For example, Saitov [62]. et al used a simple method to calculate the DOS and using our results as a supporting article they found that there is a negligible weak dependence of charge carriers' lifetime on the photon energy and they showed that the peculiarities of the absorption and photoconductivity spectra are determined mainly by the Gaussian distribution of the density of states (DOS). Therefore, they could demonstrate that DOS distribution directly influences the transport properties of the material. In the complete picture, the outcomes of this research hold a significant promise for advancing electronic device fabrication. Enabling the prediction of critical parameters across various applications, including charge transport and luminescence. Our findings offer valuable insights into enhancing device performance. Moreover, unveils the potential to observe physical phenomena that were previously obscured by disorder-induced limitations.

Adding to the complexity there is a common consideration in the field of polymer nanocomposites. When conductive nanofillers are added to a polymer matrix to enhance optical and electrical properties, it prompts the inquiry into whether the improved device performance is primarily due to the conductive nature of the nanofillers or if there are changes occurring in the polymer structures. Our second research addresses this significant question by addition of nan-conductive nanofillers with various concentrations into the polymer matrix. Based on the achieved results, this research provides insights into how non-conductive nanoparticles affect material properties and addresses whether modifying the structure of the active layer using nanofillers can bring about

specific improvements in the performance of an electronic device. We are confident that our research can contribute to optimizing polymer light sources, clarifying some of the factors influencing efficiency and lifetime of the devices. Our study provides valuable insights into the influence of non-conductive nanoparticles on both material properties and the functionality of the resulting device.

7.2 Ongoing research and Future prospects

Building on the obtained outcomes, the recent investigation centered on integrating nanoparticles into various conjugated polymers, such as F8BT and MEH-PPV. These polymers serve as a representative of conductive polymers with documented real-world applications in the electronics industry. Based on the stability and lifetime measurement results, we were able to improve charge stability and thus prolonged operating time of the PLEDs using the addition if nonconductive nanofillers into the conjugated polymer matrix. However, the electroluminescence intensity measurement that was carried out under the constant flow of electric current through the device indicted that the addition of nonconductive nanofillers reduced the luminance of the device compared to neat MEH-PPV. From a practical point of view, the improvement of luminance, stability and external quantum efficiency of devices play a significant role in the technology transfer from laboratory to real applications. In order to achieve optimal dispersion of nanoparticles within polymers and fabricate practical polymer light-emitting devices with high efficiency, there is a need for further research to improve the understanding of nanoparticle dispersion and interactions, as well as the different fabrication methods used in the production of thin film nanocomposites. This involves a comprehensive analysis of fundamental properties of nanofillers, focusing on size-dependent characteristics, quantum effects, and the intricate interplay between nanoparticles and polymer matrixes. we believe, it will be possible to find a suitable nanofiller enabling both governing of the structure and improving the luminance of devices in the future.

7.3 Publication of the results

According to the rules of Tomas Bata University in Zlín, at least a substantial part of the core of results of a dissertation shall be published in impacted journals to assure the work is examined in an independent review process and meets the criteria of current world state of the art in its field.

As such, the research work is always performed within the research group and any publication has co-authors contributing according to their role in the team. Moreover, there is also a vivid cooperation with national and foreign research teams.

The results presented in this thesis pertaining the F8BT thin films have been already published in [BG]. Specifically, in this work, ER-EIS and GIWAXS measurements were done in Bratislava at Institute of Physics of the Slovak Academy of Sciences by Dr. Vojtech Nádaždy, Dr. Karol Végsö and Dr. Peter Šiffalovič. All other work on the thin film sample preparation and spectroscopic characterization as well the data interpretation was performed by me under the auspices and with the help of my supervisor, consultant and other colleagues in the team being the co-authors of the paper.

The second and third parts of this work have been embodied into one manuscript entitled "Trade-off between high performance and long life due to nanofiller effects in polymer LEDs: MEH-PPV/Al_2O_3 nanocomposite study", which is under second review after revisions in Applied Surface Science at the time of compiling this text. Again, the ER-EIS and GIWAXS measurements were done in Bratislava, whereas the SPV and CELIV measurements were performed in Prague at the Faculty of Mathematics and Physics of the Charles University by assoc. prof. Jana Toušková and assoc. prof. Jiří Toušek. I was given the opportunity to get training and performed a part of these measurements during my stay in Prague under their supervision. Their student Patricie Klosse also contributed by conductivity measurements. Some of these measurements were also performed by my consultant Dr. Pavel Urbánek who often visited this institute. The other work on the sample preparation, namely thin films preparation, fabrication of devices, spectroscopic characterization and data interpretation were performed by me under the auspices and with the help of my supervisor, consultant and other colleagues in the team being the co-authors of the manuscript.

References

Author's article

[BG] B. Ghasemi, J. Ševčík, V. Nádaždy, K. Végsö, P. Šiffalovič, P. Urbánek, I. Kuřitka, Thickness Dependence of Electronic Structure and Optical Properties of F8BT Thin Films, Polymers (Basel). 14 (2022) 641. https://doi.org/10.3390/polym14030641.

Other references

[1] B.A. Al-Asbahi, S.M.H. Qaid, H.M. Ghaithan, W.A. Farooq, Enhancing the Optical and Optoelectronic Properties of MEH-PPV-Based Light-Emitting Diodes by Adding SiO2/TiO2 Nanocomposites, J. Non. Cryst. Solids. 552 (2021) 120429. https://doi.org/10.1016/j.jnoncrysol.2020.120429.

[2] L. Diodes, Effects of MEH-PPV Molecular Ordering in the Emitting Layer on the Luminescence Efficiency of Organic Light-Emitting Diodes, Molecules. 26 (2021) 2512. https://doi.org/10.3390/molecules26092512.

[3] S. Ashok Kumar, J.S. Shankar, B.K. Periyasamy, Study on interfacial interactions and optoelectronic properties of MEH-PPV/SnO2hetero-structure, Semicond. Sci. Technol. 37 (2022). https://doi.org/10.1088/1361-6641/ac5675.

[4] J.L. Brédas, R.R. Chance, R. Silbey, Comparative theoretical study of the doping of conjugated polymers: Polarons in polyacetylene and polyparaphenylene, Phys. Rev. B. 26 (1982) 5843–5854. https://doi.org/10.1103/PhysRevB.26.5843.

[5] and A.J.H. C. K. Chiang, C. R. Fincher, Jr., Y. W. Park, Electrical Conductivity in Doped Polyacetylene, Phys. Rev. I, ETTERS. 39 (1977) 1098–1101.

[6] C.K.C. and A.J.H. H. Shirakawa, E. J. Louis, A. G.Macdiarmid, Synthesis of electrically conducting organic polymers: halogen derivatives of polyacetylene, (CH)x, J.C.S. CHEM. COMM. (1977) 578–580.

[7] H. Sirringhaus, Device Physics of Solution-Processed Organic Field-Effect Transistors **, Adv. Energy Mater. (2005) 2411–2425. https://doi.org/10.1002/adma.200501152.

[8] Y. Woo, A.J. Heeger, Conducting polymers for carbon electronics themed issue Semiconducting polymers : the Third Generation w, Chem. Soc. Rev. 39 (2010) 2354–2371. https://doi.org/10.1039/b914956m.

[9] N.E. Jackson, B.M. Savoie, K.L. Kohlstedt, M. Olvera, D. Cruz, G.C.

Schatz, L.X. Chen, M.A. Ratner, Controlling Conformations of Conjugated Polymers and Small Molecules : The Role of Nonbonding Interactions, (2013).

[10] R. Silbey, Non-linear polamzabilities of conjugated chains: regular polyenes, solitons, and polarons, Chem. Phys. Lett. 140 (1987) 537–541. https://doi.org/doi.org/10.1016/0009-2614(87)80482-7.

[11] Z. Di Yu, Y. Lu, J.Y. Wang, J. Pei, Conformation Control of Conjugated Polymers, Chem. - A Eur. J. 26 (2020) 16194–16205. https://doi.org/10.1002/chem.202000220.

[12] F.C. Spano, Excitons in conjugated oligomer aggregates, films, and crystals, Annu. Rev. Phys. Chem. 57 (2006) 217–243. https://doi.org/10.1146/annurev.physchem.57.032905.104557.

[13] H. Yamagata, F.C. Spano, Interplay between intrachain and interchain interactions in semiconducting polymer assemblies: The HJ-aggregate model, J. Chem. Phys. 136 (2012) 184901. https://doi.org/10.1063/1.4705272.

[14] H. Yamagata, N.J. Hestand, F.C. Spano, A. Köhler, C. Scharsich, S.T. Hoffmann, H. Bässler, The red-phase of poly[2-methoxy-5-(2-ethylhexyloxy)- 1,4-phenylenevinylene] (MEH-PPV): A disordered HJ-aggregate, J. Chem. Phys. 139 (2013). https://doi.org/10.1063/1.4819906.

[15] F.C. Spano, C. Silva, H- and J-aggregate behavior in polymeric semiconductors, Annu. Rev. Phys. Chem. 65 (2014) 477–500. https://doi.org/10.1146/annurev-physchem-040513-103639.

[16] C. Hellmann, F. Paquin, N.D. Treat, A. Bruno, L.X. Reynolds, S.A. Haque, P.N. Stavrinou, C. Silva, N. Stingelin, Controlling the interaction of light with polymer semiconductors, Adv. Mater. 25 (2013) 4906–4911. https://doi.org/10.1002/adma.201300881.

[17] F. Schindler, J. Jacob, A.C. Grimsdale, U. Scherf, K. Müllen, J.M. Lupton, J. Feldmann, Counting chromophores in conjugated polymers, Angew. Chemie - Int. Ed. 44 (2005) 1520–1525. https://doi.org/10.1002/anie.200461784.

[18] R. Lécuiller, J. Berréhar, J.D. Ganière, J.D. Ganière, C. Lapersonne-Meyer, P. Lavallard, M. Schott, Fluorescence yield and lifetime of isolated polydiacetylene chains: Evidence for a one-dimensional exciton band in a conjugated polymer, Phys. Rev. B - Condens. Matter Mater. Phys. 66 (2002) 1252051–1252056. https://doi.org/10.1103/PhysRevB.66.125205.

[19] M. Kasha, Energy transfer mechanisms and the molecular exciton model for molecular aggregates, Radiat. Res. 178 (2012) 55–70. https://doi.org/10.1667/RRAV03.1.

[20] H. Yamagata, F.C. Spano, Strong photophysical similarities between conjugated polymers and J-aggregates, J. Phys. Chem. Lett. 5 (2014) 622–632. https://doi.org/10.1021/jz402450m.

[21] H. Fidder, J. Knoester, D.A. Wiersma, Superradiant emission and optical dephasing in J-aggregates, Chem. Phys. Lett. 171 (1990) 529–536. https://doi.org/10.1016/0009-2614(90)85258-E.

[22] F.P. Diehl, C. Roos, A. Duymaz, B. Lunkenheimer, A. Köhn, T. Basché, Emergence of coherence through variation of intermolecular distances in a series of molecular dimers, J. Phys. Chem. Lett. 5 (2014) 262–269. https://doi.org/10.1021/jz402512g.

[23] F. Dubin, R. Melet, T. Barisien, R. Grousson, L. Legrand, M. Schott, V. Voliotis, Macroscopic coherence of a single exciton state in an organic quantum wire, Nat. Phys. 2 (2006) 32–35. https://doi.org/10.1038/nphys196.

[24] H. Yamagata, F.C. Spano, Vibronic coupling in quantum wires: Applications to polydiacetylene, J. Chem. Phys. 135 (2011) 054906. https://doi.org/10.1063/1.3617432.

[25] N.R. Conley, A.K. Pomerantz, H. Wang, R.J. Twieg, W.E. Moerner, Bulk and single-molecule characterization of an improved molecular beacon utilizing H-dimer excitonic behavior, J. Phys. Chem. B. 111 (2007) 7929–7931. https://doi.org/10.1021/jp073310d.

[26] J. Clark, C. Silva, R.H. Friend, F.C. Spano, Role of intermolecular coupling in the photophysics of disordered organic semiconductors: Aggregate emission in regioregular polythiophene, Phys. Rev. Lett. 98 (2007) 1–4. https://doi.org/10.1103/PhysRevLett.98.206406.

[27] S.P. Jagtap, S. Mukhopadhyay, V. Coropceanu, G.L. Brizius, J.L. Brédas, D.M. Collard, Closely stacked oligo(phenylene ethynylene)s: Effect of π-stacking on the electronic properties of conjugated chromophores, J. Am. Chem. Soc. 134 (2012) 7176–7185. https://doi.org/10.1021/ja3019065.

[28] T. Stangl, P. Wilhelm, D. Schmitz, K. Remmerssen, S. Henzel, S.S. Jester, S. Höger, J. Vogelsang, J.M. Lupton, Temporal fluctuations in excimer-like interactions between π-conjugated chromophores, J. Phys. Chem. Lett. 6 (2015) 1321–1326. https://doi.org/10.1021/acs.jpclett.5b00328.

[29] M. Ilton, Flow in thin polymer films, Ph.D. Thesis. (2015) 143.

[30] F. Bächle, C. Maichle-Mössmer, T. Ziegler, Helical Self-Assembly of Optically Active Glycoconjugated Phthalocyanine J-Aggregates, Chempluschem. 84 (2019) 1081–1093. https://doi.org/10.1002/cplu.201900381.

[31] J. Wang, S. Kaskel, KOH activation of carbon-based materials for energy storage, J. Mater. Chem. 22 (2012) 23710–23725. https://doi.org/10.1039/c2jm34066f.

[32] S. Wang, C. Xiao, Y. Xing, H. Xu, S. Zhang, Carbon nanofibers/nanosheets hybrid derived from cornstalks as a sustainable anode for Li-ion batteries, J. Mater. Chem. A. 3 (2015) 6742–6746. https://doi.org/10.1039/c5ta00050e.

[33] M.A. Salam, M. Mokhtar, S.N. Basahel, S.A. Al-Thabaiti, A.Y. Obaid, Removal of chlorophenol from aqueous solutions by multi-walled carbon nanotubes: Kinetic and thermodynamic studies, J. Alloys Compd. 500 (2010) 87–92. https://doi.org/10.1016/j.jallcom.2010.03.217.

[34] Muhammad Hafeez, Recent Progress and Overview of Nanocomposites, Nanocomposite Mater. Biomed. Energy Storage Appl. (2022). https://doi.org/10.5772/intechopen.102469.

[35] T.A. Saleh, N.P. Shetti, M.M. Shanbhag, K. Raghava Reddy, T.M. Aminabhavi, Recent trends in functionalized nanoparticles loaded polymeric composites: An energy application, Mater. Sci. Energy Technol. 3 (2020) 515–525. https://doi.org/10.1016/j.mset.2020.05.005.

[36] S. Paszkiewicz, K. Pypeć, I. Irska, E. Piesowicz, Functional polymer hybrid nanocomposites based on polyolefins: A review, Processes. 8 (2020) 1–13. https://doi.org/10.3390/pr8111475.

[37] Q. Fang, K. Lafdi, Effect of nanofiller morphology on the electrical conductivity of polymer nanocomposites, Nano Express. 2 (2021). https://doi.org/10.1088/2632-959X/abe13f.

[38] N. Ali, B. Zhang, H. Zhang, W. Zaman, W. Li, Q. Zhang, Key synthesis of magnetic Janus nanoparticles using a modified facile method, Particuology. 17 (2014) 59–65. https://doi.org/10.1016/j.partic.2014.02.001.

[39] K. Saeed, I. Khan, Preparation and characterization of functionalized multiwalled carbon nanotubes filled polyethylene oxide nanocomposites, J. Rubber Res. 23 (2020) 187–192. https://doi.org/10.1007/s42464-020-00048-6.

[40] E.M. Masoud, L. Liu, B. Peng, Synthesis, characterization, and applications of polymer nanocomposites, J. Nanomater. 2020 (2020) 10–12. https://doi.org/10.1155/2020/5439136.

[41] N. Ali, B. Zhang, H. Zhang, W. Zaman, S. Ali, Z. Ali, W. Li, Q. Zhang, Monodispers and Multifunctional Magnetic Composite Core Shell Microspheres for Demulsification Applications, J. Chinese Chem. Soc. 62 (2015) 695–702. https://doi.org/10.1002/jccs.201500151.

[42] P.L.B.& A.B.H. J. H. Burroughes, D. D. C. Bradley, A. R. Brown, R. N. Marks, K. Mackay, R. H. Friend, Lightemitting-Diodes-Based-on-Conjugated-Polymers-1990, (1990) 539–541.

[43] J.M. Fuhrman Kirk; Davis, Allinson, Flexible light-emitting diodes made from soluble conducting polymers, Nature. 359 (1992) 710–713.

[44] J. Kido, K. Hongawa, K. Okuyama, K. Nagai, White light-emitting organic electroluminescent devices using the poly(N-vinylcarbazole) emitter layer doped with three fluorescent dyes, Appl. Phys. Lett. 64 (1994) 815–817. https://doi.org/10.1063/1.111023.

[45] M. F. Rahman, M. Moniruzzaman, Fundamentals of Organic Light Emitting Diode, Sci. Technol. Conf. (2015) 1–6.

[46] H. Peng, X. Sun, W. Weng, X. Fang, Light Emitting Based on Polymer, Polym. Mater. Energy Electron. Appl. (2017) 243–285. https://doi.org/10.1016/b978-0-12-811091-1.00007-0.

[47] P. Urbanek, I. Kuritka, S. Danis, J. Touskova, J. Tousek, Thickness threshold of structural ordering in thin MEH-PPV films, Polymer (Guildf). 55 (2014) 4050–4056. https://doi.org/10.1016/j.polymer.2014.05.054.

[48] Y. Xiong, J.B. Peng, H. Bin Wu, J. Wang, Improved performance of polymer light-emitting diodes with an electron transport emitter by post-annealing, Chinese Phys. Lett. 26 (2009). https://doi.org/10.1088/0256-307X/26/9/097801.

[49] P. Urbánek, I. Kuřitka, Thickness dependent structural ordering, degradation and metastability in polysilane thin films: A photoluminescence study on representative σ-conjugated polymers, J. Lumin. 168 (2015) 261–268. https://doi.org/10.1016/j.jlumin.2015.08.022.

[50] P. Urbánek, I. Kuřitka, J. Ševčík, J. Toušková, J. Toušek, V. Nádaždy, P. Nádaždy, K. Végsö, P. Šiffalovič, R. Rutsch, M. Urbánek, An experimental and theoretical study of the structural ordering of the PTB7 polymer at a mesoscopic scale, Polymer (Guildf). 169 (2019) 243–254. https://doi.org/10.1016/j.polymer.2019.02.048.

[51] C.L. Donley, J. Zaumseil, J.W. Andreasen, M.M. Nielsen, H. Sirringhaus, R.H. Friend, J.S. Kim, Effects of packing structure on the optoelectronic and charge transport properties in poly(9,9-di-n-octylfluorene-alt-benzothiadiazole), J. Am. Chem. Soc. 127 (2005) 12890–12899. https://doi.org/10.1021/ja051891j.

[52] E.K. Miller, D. Yoshida, C.Y. Yang, A.J. Heeger, Polarized ultraviolet absorption of highly oriented poly„2-methoxy, 5-„28-ethyl…-hexyloxy… paraphenylene vinylene, Phys. Rev. B. 59 (1999) 4661–4664.

[53] D.L. Wood, Weak Absorption Tails in Amorphous Semiconductors, Phys. Rev. B. 5 (1972) 3144–3151.

[54] N.Y. Zayana, S.S. Shariffudin, N.S. Jumali, Z. Shaameri, A.S. Hamzah, M. Rusop, Optical properties of MEH-PPV, AIP Conf. Proc. 1328 (2011) 271–273. https://doi.org/10.1063/1.3573751.

[55] P. Urbánek, I. Kuřitka, S. Daniš, J. Toušková, J. Toušek, Thickness threshold of structural ordering in thin MEH-PPV films, Polymer (Guildf). 55 (2014) 4050–4056. https://doi.org/10.1016/j.polymer.2014.05.054.

[56] O. Mirzov, I.G. Scheblykin, Photoluminescence spectra of a conjugated polymer : from films and solutions to single molecules, Phys. Chem. Chem. Phys. 8 (2006) 5569–5576. https://doi.org/10.1039/b612073c.

[57] R. Noriega, J. Rivnay, K. Vandewal, F.P.V. Koch, N. Stingelin, P. Smith, M.F. Toney, A. Salleo, A general relationship between disorder, aggregation and charge transport in conjugated polymers, Nat. Mater. 12 (2013) 1038–1044. https://doi.org/10.1038/nmat3722.

[58] J. Toušek, J. Toušková, Z. Remeš, J. Cˇermák, J.K. A, D.K. B, I. Kurˇitka, Exciton diffusion length and concentration of holes in MEH-PPV polymer using the surface voltage and surface photovoltage methods, Chem. Phys. Lett. 552 (2012) 49–52. https://doi.org/10.1016/j.cplett.2012.09.052.

[59] C.A. Amorim, M.R. Cavallari, G. Santos, F.J. Fonseca, A.M. Andrade, S. Mergulhão, Determination of carrier mobility in MEH-PPV thin-films by stationary and transient current techniques, J. Non. Cryst. Solids. 358 (2012) 484–491. https://doi.org/10.1016/J.JNONCRYSOL.2011.11.001.

[60] J.C. Scott, J.H. Kaufman, P.J. Brock, R. DiPietro, J. Salem, J.A. Goitia, Degradation and failure of MEH-PPV light-emitting diodes, J. Appl. Phys. 79 (1996) 2745–2751. https://doi.org/10.1063/1.361096.

[61] T. Jamatia, D. Skoda, P. Urbanek, J. Sevcik, J. Maslik, L. Munster, L. Kalina, I. Kuritka, Microwave-assisted synthesis of FexZn1−xO nanoparticles for use in MEH-PPV nanocomposites and their application in polymer light-emitting diodes, J. Mater. Sci. Mater. Electron. 30 (2019) 11269–11281. https://doi.org/10.1007/s10854-019-01473-z.

[62] S.R. Saitov, D.N. Litvinenko, A.E. Aleksandrov, O. V. Snigirev, A.R. Tameev, A.M. Smirnov, V.N. Mantsevich, Spectral (in)dependence of nonequilibrium charge carriers lifetime and density of states distribution in the vicinity of the band gap edge in F8BT polymer, Appl. Phys. Lett. 123 (2023). https://doi.org/10.1063/5.0156576.

List of figures

List of tables

List of symbols, acronyms and abbreviations used

AFM Atomic-force microscopy

CP Conjugated polymer

DOS Density of states

ER-EIS Energy-resolved Electrochemical impedance spectroscopy

ETL Electron transporting layer

HJ Hetero-junction

HOMO Highest occupied molecular orbital

HTL Hole transporting layer

ETL Electron transporting layer

ITO Indium tin oxide

I-V Current voltage

LED Light-emitting diode

LEP Light emitting polymer

LUMO Lowest unoccupied molecular orbital

MOSFET Metal-oxide-semiconductor field-effect transistor

OFET Organic field-effect transistors

OLED Organic light-emitting diode

OPD Organic photodetectors

OPV Organic photovoltaic

OSC Organic semiconductor

PL Photoluminescence

PLED Polymer light-emitting diode

SCR Space-charge region

SPV Surface photovoltage

TLC Trap-limited current

GIWXAS Grazing-incidence wide-angle X-ray scattering

CELIV Charge extraction by linearly increasing voltage

Author's professional Curriculum Vitae

Personal information:

Name: Bita Ghasemi

Date of birth: 20/09/1985

Place of birth: Kermanshah, Iran

Address: Stefanikova 150

Affiliation University: Centre of Polymer Systems, Tomas Bata in Zlín, třída Tomáše Bati 5678, 760 01 Zlín

Email: ghasemi@utb.cz

Education:

Ph.D. studies in Nanotechnology and advanced Materials (2019-Present)

Center of Polymer Systems, Tomas Bata University in Zlin , Czech Republic

Thesis: Preparation and characterization of nanocomposite thin films for polymer electronics

MSc, Physics (Solid State) ***(Sept. 2012 – Aug. 2014)***

Azad University of Karaj, Karaj, Iran

Thesis: Investigation of nano- structural and optical properties of molybdenum nitride thin films prepared at different deposition conditions on quartz substrates

BSc, Physics (Solid State) ***(Sept. 2004 – Sept. 2008)***

Hamedan Azad University, Hamedan, Iran

List of publications by the author

Journal Publications

1. **Ghasemi, Bita**; Hajakbari, Fatemeh; Hojabri, Alireza. 2020. "Structural and optical properties of nanocrystalline MoO3 thin films grown by thermal oxidation of sputtered molybdenum films". Inorganic and Nano-Metal Chemistry, Volume 50, Issue 5, Pages 414-422, https://www.tandfonline.com/doi/full/10.1080/24701556.2020.1716008
2. Sevcik, Jakub; Urbánek, Pavel; Hanulikova, Barbora; Čapková, Tereza; Urbánek, Michal; Antoš, Jan; Londesborough, Michael G. S.; Bould, Jonathan; **Ghasemi, Bita**; Petřkovský, Lukáš; Kuřitka, Ivo. 2021."The Photostability of Novel Boron Hydride Blue Emitters in Solution and Polystyrene Matrix". Materials, Volume 14, Issue 3, 589, https://doi.org/10.3390/ma14030589
3. **Ghasemi, Bita**; Ševčík, Jakub; Nádaždy, Vojtech; Végsö, Karol; Šiffalovič, Peter; Urbánek, Pavel; Kuřitka, Ivo. 2022. "Thickness Dependence of Electronic Structure and Optical Properties of F8BT Thin Films". Polymers, Volume 14, Issue 3, 641, https://www.mdpi.com/2073-4360/14/3/641/htm
4. **Ghasemi, Bita**; Ševčík, Jakub; Toušková, Jana; Toušek, Jiří; Klosse, Patricie; Nádaždy, Vojtěch; Végso, Karol; Šiffalovič, Peter; Hanulíková, Barbora; Urbánek, Michal; Kuřitka, Ivo and Urbánek, Pavel; "Trade-off between high performance and long life due to nanofiller effects in polymer LEDs: MEH-PPV/Al_2O_3 nanocomposite study". Applied Surface Science, Volume 657, 159807, https://doi.org/10.1016/j.apsusc.2024.159807

Conference Publications

1. **Bita Ghasemi**; Pavel Urbanek; Ivo Kuřitka. April 25-28, 2022. "Boosting LED performance by structural disorder induced by Al2O3 nanofiller in MEH-PPV active layer". 5th International Conference on Applied Surface Science, Palma, Mallorca, Spain, EU.
2. **Bita Ghasemi**; Jakub Ševčík; Pavel Urbanek; Ivo Kuřitka. October 21-23, 2020. "Polymer chain ordering manifestation in photoluminescence of thin F8BT films". 12th International Conference on Nanomaterials-Research and Application, Brno, Czech Republic, EU,

https://scholar.google.com/citations?view_op=view_citation&hl=en&user=SbPlvcEAAAAJ&citation_for_view=SbPlvcEAAAAJ:u-x6o8ySG0sC

3. **Bita Ghasemi**; Fatemeh Hajakbari; Alireza Hojabri. 2015. “Effect of deposition power on nanostructure and optical properties of molybdenum nitride thin films”. 12th Conference on Condensed Matter, Physics Society of Iran, Isfahan University of Technology.
4. **Bita Ghasemi**; Fatemeh Hajakbari; Alireza Hojabri. 2015. “Study of the structural and morphological properties of molybdenum nitride thin films prepared at different deposition times”. The Second National Conference on Mathematics and Physics, University of Tehran.

Technical Internship

Internship in Charles University at the faculty of Mathematics and Physics at the department of Macromolecule Physics, Prague, 14/03 to 25/03, 2022

Internship at the University of Edinburgh, School of Engineering, United Kingdom, 20/04 to 12/07, 2023

Projects

1. IGA/CPS/2020/003 - "Preparation and characterization of nanocomposite systems", member of the research team.
2. IGA/CPS/2021/002 - "Preparation and characterization of nanocomposite systems", member of the research team.
3. IGA/CPS/2022/002 - "Preparation and characterization of nanocomposite systems", member of the research team.
4. IGA/CPS/2023/006-"Preparation and characterization of nanocomposite systems", member of the research team.

Preparation and characterization of nanocomposite thin films for polymer electronics

Preparation and characterization of nanocomposite thin films for polymer electronics

Doctoral Thesis Summary

Published by: Tomas Bata University in Zlín,

nám. T. G. Masaryka 5555, 760 01 Zlín.

Edition: published electronically

Typesetting by: Bita Ghasemi

This publication has not undergone any proofreading or editorial review.

Publication year: 2024

First Edition

ISBN 978-80-7678-257-0